Graphical Abstract

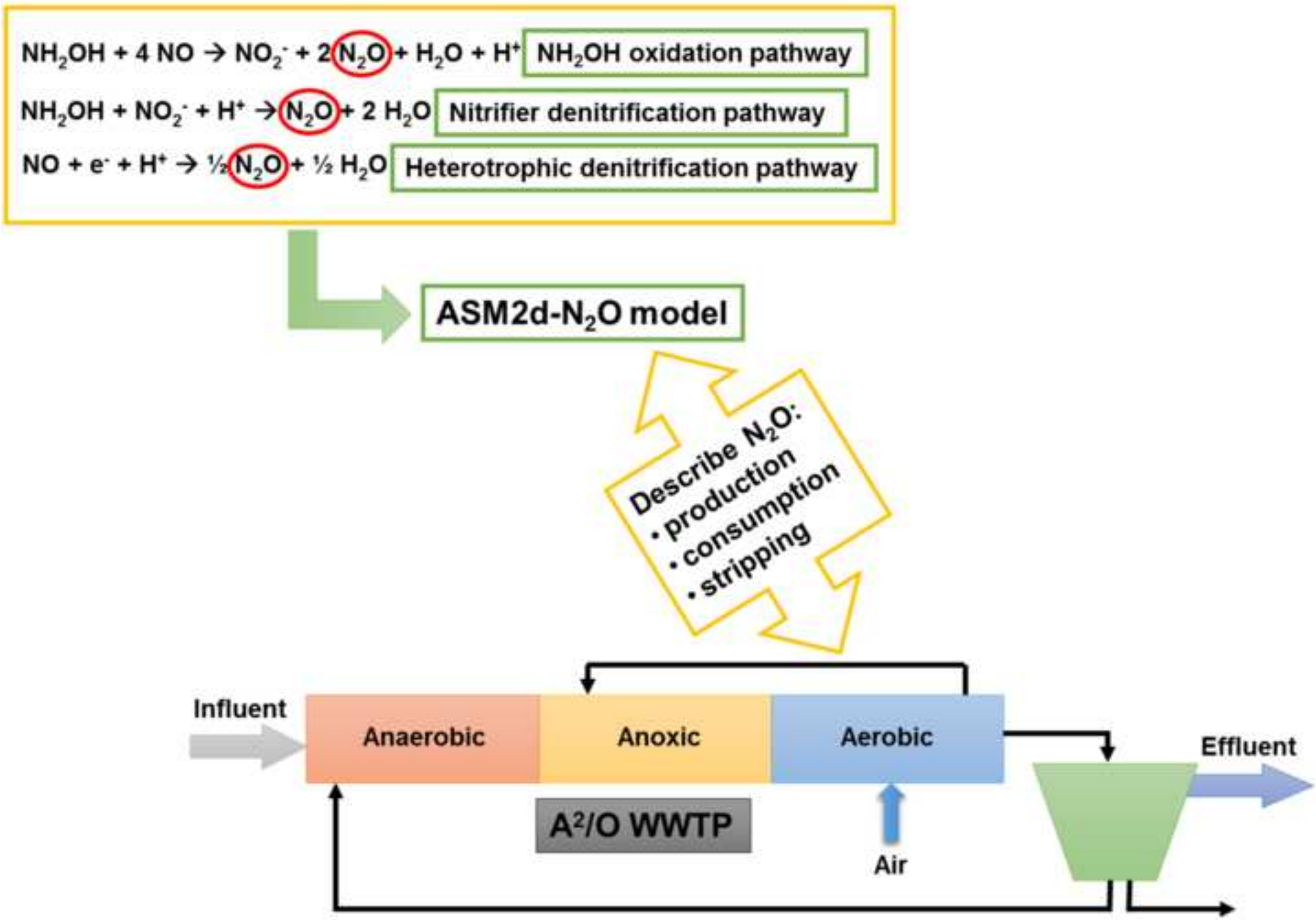

Highlights

- N_2O mitigation calls for the modeling of all production pathways under changing DO.
- If complete nitrification occurs, low aeration decreases the WWTP carbon footprint.
- Partial nitrification combined with high stripping caused the highest N_2O emission.

Development of an ASM2d-N_2O model to describe nitrous oxide emissions in municipal WWTPs under dynamic conditions

Theoni Maria Massara [a,b], Borja Solís [c], Albert Guisasola [c], Evina Katsou [a,b], Juan Antonio Baeza [c]

[a] Department of Mechanical, Aerospace and Civil Engineering, Brunel University London, Uxbridge Campus, Middlesex, UB8 3PH, Uxbridge, UK.

[b] Institute of Environment, Health and Societies, Brunel University London, Kingston Lane, Middlesex, UB8 3PH, Uxbridge, UK.

[c] GENOCOV. Departament d'Enginyeria Química, Biològica i Ambiental, Escola d'Enginyeria, Universitat Autònoma de Barcelona, Cerdanyola del Vallés (Barcelona), 08193, Barcelona, Spain.

Corresponding Author:

Prof. Juan Antonio Baeza,

Email: JuanAntonio.Baeza@uab.cat, Tel.: +34 93 581 1587

Abstract

Nitrous oxide (N_2O), a significant contributor to the greenhouse effect, is generated during the biological nutrient removal in wastewater treatment plants (WWTPs). Developing mathematical models estimating the N_2O dynamics under changing operational conditions (e.g. dissolved oxygen, DO) is essential to design mitigation strategies. Based on the activated sludge models (ASM) structure, this work presents an ASM2d-N_2O model including all the biological N_2O production pathways for a municipal WWTP under an anaerobic/anoxic/oxic (A^2/O) configuration with biological removal of organic matter, nitrogen and phosphorus, and its application in different dynamic scenarios. Three microbial N_2O production pathways were considered: nitrifier denitrification, hydroxylamine oxidation, and heterotrophic denitrification, with the first two being activated by ammonia oxidizing bacteria (AOB). A stripping effectivity (SE) coefficient was added to reflect the non-ideality of the stripping modeling. With the DO in the aerobic compartment ranging from 1.8 to 2.5 mg L^{-1}, partial nitrification and high N_2O production via nitrifier denitrification were noted, indicating that low aeration strategies lead to a low overall carbon footprint only if complete nitrification is not hindered. High N_2O emissions were predicted as a combination of low DO (~1.1 mg L^{-1}) with high ammonium concentration. With the AOB prevailing over the Nitrite Oxidizing Bacteria (NOB), nitrite was accumulated, thus activating the nitrifier denitrification pathway. After suddenly increasing the influent ammonium load, the AOB had a greater growth compared to the NOB and the same pathway was considered as N_2O hotspot. Especially under conditions promoting partial nitrification (i.e. low DO) and raising the stripping effect importance (i.e. high SEs), the highest N_2O emission factors were predicted.

Keywords A^2/O, nitrous oxide, emission factor, modeling, N_2O production pathways, N_2O stripping

Abbreviations

A^2/O	Anaerobic/Anoxic/Oxic WWTP configuration
AOB	Ammonia Oxidizing Bacteria
AOR	Ammonium Oxidation Rate
ASM	Activated Sludge Models
ASMN	Activated Sludge Model for Nitrogen
BNR	Biological Nutrient Removal
C	Carbon
COD	Chemical Oxygen Demand
DO	Dissolved Oxygen
EF	Emission Factor
EBPR	Enhanced Biological Phosphorus Removal
GHG	Greenhouse Gas
GWP	Global Warming Potential
HRT	Hydraulic Retention Time
IWA	International Water Association
N	Nitrogen
NOB	Nitrite Oxidizing Bacteria
OHO	Ordinary Heterotrophic Organisms
P	Phosphorus
PAO	Phosphorus Accumulating Organisms
PHA	Polyhydroxyalkanoates
PP	Polyphosphates
SA	Sensitivity Analysis
SBR	Sequencing Batch Reactor
SE	Stripping Effectivity
TKN	Total Kjeldahl Nitrogen
TSS	Total Suspended Solids
WWTP	Wastewater Treatment Plant

1. Introduction

Nitrous oxide (N_2O) is a particularly important greenhouse gas (GHG) because of its high global warming potential (GWP) compared to other GHGs such as methane (CH_4) and carbon dioxide (CO_2). N_2O has a GWP 265 times higher than CO_2, in contrast to CH_4 that has a GWP only 28 times higher than CO_2 [1]. Moreover, N_2O has been characterized as the predominant ozone-depleting substance of the century [2]. N_2O can be produced and directly emitted during the biological nutrient removal (BNR) in wastewater treatment plants (WWTPs) [3-4]. More importantly, it has been proved that the total carbon (C) footprint of full-scale WWTPs can be affected by N_2O emissions to an impressive extent: e.g. around 60% [5], or even around 75% [6].

The currently known microbial pathways for N_2O production during the BNR are connected to the biochemical processes of nitrification and denitrification. Those related to nitrification occur through the activity of the ammonia oxidizing bacteria (AOB) (i.e. the nitrifier denitrification and the hydroxylamine (NH_2OH) oxidation). Heterotrophic denitrification, during which N_2O is an intermediate product, is the third biological pathway [5, 7-9]. The parameters mostly contributing to the N_2O generation have been reviewed and linked to insufficient levels of dissolved oxygen (DO) at the nitrification stage, increased nitrite (NO_2^-) concentration during both nitrification and denitrification, in addition to low chemical oxygen demand to nitrogen ratio (COD/N) during denitrification [10-12].

Studies have revealed a considerable variation in the N_2O emission in WWTPs, thus rendering the emission factor (EF) estimation difficult. For example, Law et al. [13] reported an EF range of 0-25% amongst different full-scale WWTPs. The significant variation can be explained through the highly dynamic conditions in WWTPs, as well as the different configurations and operational conditions applied in each plant [13-14]. Furthermore, the N_2O EF calculation can be

influenced by the N_2O quantification method [13, 15]. After examining twelve different WWTPs in the United States, Ahn et al. [3] found that the EFs ranged from 0.01 to 1.8% when normalized to the influent Total Kjeldahl Nitrogen (TKN) load. This variability was correlated with the diurnal variations of the influent N-loading. Similarly, Rodriguez-Caballero et al. [16] examined the N_2O dynamics in a municipal WWTP. Due to instable nitrification in the bioreactor, the emissions presented a significant decreasing trend within the day; the reported N_2O EF decreased from 0.116 to 0.064% of the influent TKN. In both cases, the authors captured the changing N_2O dynamics because of the continuous online reporting of the data. Foley et al. [4] studied seven full-scale BNR WWTPs in Australia with various configurations, concluding to a minimum N_2O EF of 0.6% and a maximum of 25.3% of the N-denitrified. The authors recommended online emission monitoring in the biological compartments for the in-depth understanding of the influent dynamics and process characteristics in WWTPs. Daelman et al. [6] examined different monitoring scenarios on a 16-month dataset of a fully covered WWTP in the Netherlands to conclude to the most accurate and cost-effective one. The estimation of the average annual N_2O emission required the description of seasonal dynamics and, thus, the acquisition of long-term, online or grab samples (the latter including nightly and weekend sampling). On the other hand, short-term campaigns focusing on the diurnal trends proved to be more expensive since they called for high-frequency online sampling. Thus, the accurate estimation of the N_2O EF within a WWTP is a highly challenging task depending on various factors such as the operational conditions, the configuration type, the quantification method, the sampling strategy, etc.

The development of mathematical tools for the prediction of N_2O emissions during the operation of WWTPs seems essential to allow the study of different scenarios. The simulation of N_2O production allows the optimization of BNR processes, thus facilitating the decrease of N_2O

emissions. N_2O modeling is constantly advancing; models describing different pathways and based on different assumptions have been developed [9, 17].

For instance, models that focus on the nitrifier denitrification pathway have been suggested: Ni et al. [18] developed a model describing how low DO levels (i.e. ≤1.5 mg L^{-1}) can inhibit complete nitrification, induce NO_2^- accumulation and, subsequently, increase N_2O emissions. Similarly, Mampaey et al. [19] observed that N_2O production and emission was mainly observed during the aerated phases under relatively low DO (i.e. ≤1.5 mg L^{-1}). The NH_2OH oxidation pathway was the basis for the models by Law et al. [20] and Ni et al. [21]. Law et al. [20] observed the N_2O production rate increasing with the ammonium oxidation rate (AOR) within an enriched AOB culture. The simulations by Ni et al. [21] indicated that ammonium (NH_4^+) accumulation during aeration was translated into a high specific AOR and, finally, into the increased production of by-products such as NH_2OH.

Given that the AOB pathways are regarded as major contributors to the N_2O production amongst the three microbial routes [7, 17, 22], 2-(AOB) pathway models have emerged. For example, the Ni et al. [23] model which depicted the following trends: (i) NH_2OH oxidation predominance under extremely low/high NO_2^- concentration along with high DO, and (ii) nitrifier denitrification predominance at low DO with moderate NO_2^- accumulation. In the 2-AOB pathway model by Pocquet et al. [17], the DO increase was combined with decreased N_2O emission along with a slightly higher contribution of the NH_2OH oxidation pathway.

Regarding the heterotrophic denitrification pathway, the activated sludge model for nitrogen (ASMN) developed by Hiatt and Grady [24] described denitrification as a four-step reaction with different specific growth rates. In a more recent model, Pan et al. [25] considered the electron

competition amongst the four heterotrophic denitrification steps by dissociating the C-oxidation and the N-reduction.

Nevertheless, N_2O is likely to be produced/consumed by both the AOB and the heterotrophic denitrifiers during the BNR in WWTPs. As a result, the development of models including all the possible pathways gives a deeper insight into the N_2O production/consumption dynamics and enhances the study of strategies for the N_2O emission mitigation, especially in cases of full-scale modeling [9-10, 12]. With the view to investigating the significant spatial variations in the N_2O flux of a step-feed 2-pass full-scale activated sludge plant, Ni et al. [26] combined the 2-(AOB) pathway modeling part by Ni et al. [23] and the heterotrophic denitrification processes appearing in Ni et al. [21] in an integrated model.

Multiple-pathway models seem more apt to elucidate the effect of changing operational parameters (e.g. DO, NO_2^- concentration, etc.) and explain possible spatial/temporal variations, thus helping plant operators with designing mitigation strategies [12]. Given the influence of aeration and DO profiles on the emissions, it is necessary to develop even more integrated models which include all the production pathways and, simultaneously, consider the N_2O transfer from the liquid to the gas phase under varying gas flow patterns.

The activated sludge models (ASM) introduced by the International Water Association (IWA) task group have been widely used for the description of BNR processes during wastewater treatment [12]. Extensions to these models have been made to consider the N_2O production with emphasis either on the nitrifier denitrification or the NH_2OH oxidation pathway, and on the impact of changing influent (e.g. influent N-loading, COD/N) and/or operational conditions (e.g. DO) [18, 21]. Nevertheless, these models lack consideration of other nutrients removal (e.g. P). Moreover, they do not necessarily pay equal attention to all biological N_2O production routes

and/or deal with the N_2O stripping modeling. Hence, the aim of this work was to develop an ASM-type model which: (i) includes N, P and organic matter removal, (ii) integrates all the microbial pathways for N_2O production/consumption, (iii) contains N_2O stripping modeling, and (iv) estimates the N_2O EF under different DO levels. To this end, the IWA ASM2d model was modified and expanded into an ASM2d-N_2O model to include all the biological N_2O production pathways and the calculation of the N_2O EF. The continuity of the model was also examined to detect typing and/or conceptual errors, inconsistencies and gaps in the proposed model. Finally, sensitivity analysis (SA) was performed to reveal the parameters most sensitive to the N_2O EF as estimated using the proposed model.

2. Materials and methods

2.1 Brief description of the WWTP configuration and influent data

The kinetic model was developed to describe the simultaneous N, P and COD removal for a WWTP with three continuous stirred tank reactors and one settler operating as an anaerobic-anoxic-aerobic (A^2/O) configuration (Fig. 1).

The first reactor (Hydraulic Retention Time: HRT=1.6 h) was anaerobic with the view to facilitating the phosphorus accumulating organisms (PAO) predominance over the ordinary heterotrophic organisms (OHO) and, subsequently, enhancing the P-removal. Nitrate (NO_3^-) entering the second (anoxic) reactor (HRT=1.6 h) through the internal recycle of the mixed liquor was denitrified by the OHO or the denitrifying PAO. Finally, the third (aerobic) reactor (HRT=5 h) coupled P and organic matter removal along with nitrification. After settling the treated effluent, the settler (HRT=2.9 h) produced two streams; the effluent and an external

recycle of biomass returned to the first reactor. The total WWTP HRT was 11.1 h, and the purge, internal and external recirculation ratios with respect to the influent flowrate were equal to 0.007, 2 and 1/3, respectively. The typical DO control setpoints for the three reactors were: 0 mg L^{-1} (anaerobic and anoxic) and 3 mg L^{-1} (aerobic).

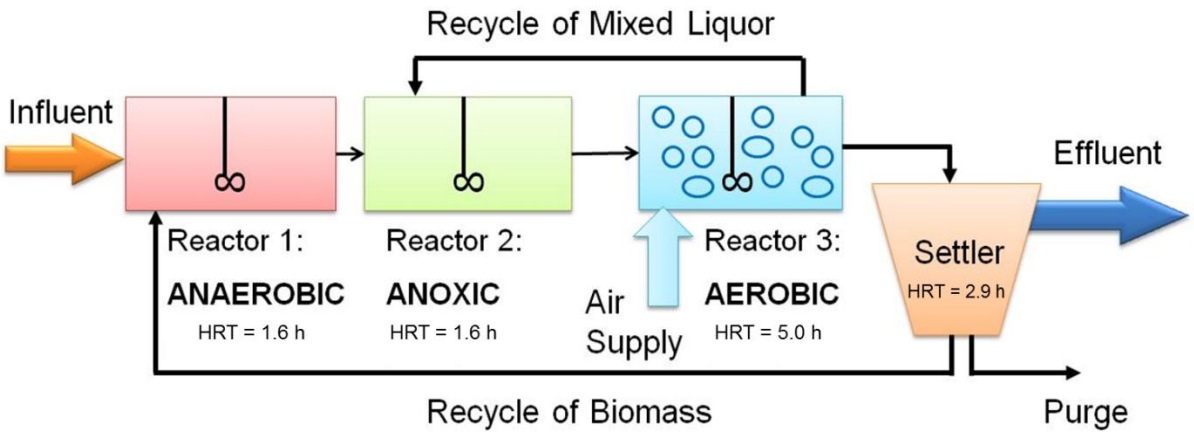

Figure 1. A^2/O WWTP configuration integrated in the current study (adapted from Guerrero et al. [27]).

The influent composition was typical for the municipal WWTP of Manresa (Catalonia, Spain) (Machado et al. [28]). The influent characterization considered S_I (inert soluble material), X_I (inert particulate organic material), X_S (slowly biodegradable substrates), and S_F (fermentable, readily biodegradable organic substrates) fractions as follows: S_I=0.07*COD, X_I=0.11*COD, X_S=0.6*COD, and S_F= 0.4*COD (Machado et al. [28]). All the remaining COD state variables were fixed to zero. The influent composition is shown in Table 1.

Table 1. Influent composition (pH=7 and T=20 ºC)

Composition	mg L^{-1}
$N\text{-}NH_4^+$	20
BOD_5	170
COD	420
Total N	35
$N\text{-}NO_3^-$	2.6
$P\text{-}PO_4^{3-}$	9
TKN (Kjeldahl N)	33
TSS	189

2.2 Model description

The core of our ASM2d-N_2O model emerged as an extension of the IWA ASM2d (i.e. an ASM version including the bioprocesses related to the heterotrophic biomass, the PAO and the nitrifiers) [29]. The scope of this study was to describe the N_2O production/consumption dynamics within a WWTP with enhanced biological phosphorus removal (EBPR). In that sense, the assumptions for the description of the two AOB pathways were made upon the Pocquet et al. [17] model, while those for the heterotrophic denitrification upon the Hiatt and Grady [24] model, always by extending and adapting the same processes to PAOs. It was considered as a holistic approach for the description of the N_2O dynamics during the BNR in WWTPs. Thus, the final model describes the following: N_2O production through all the three microbial pathways, but also N_2O consumption during denitrification (Fig. 2).

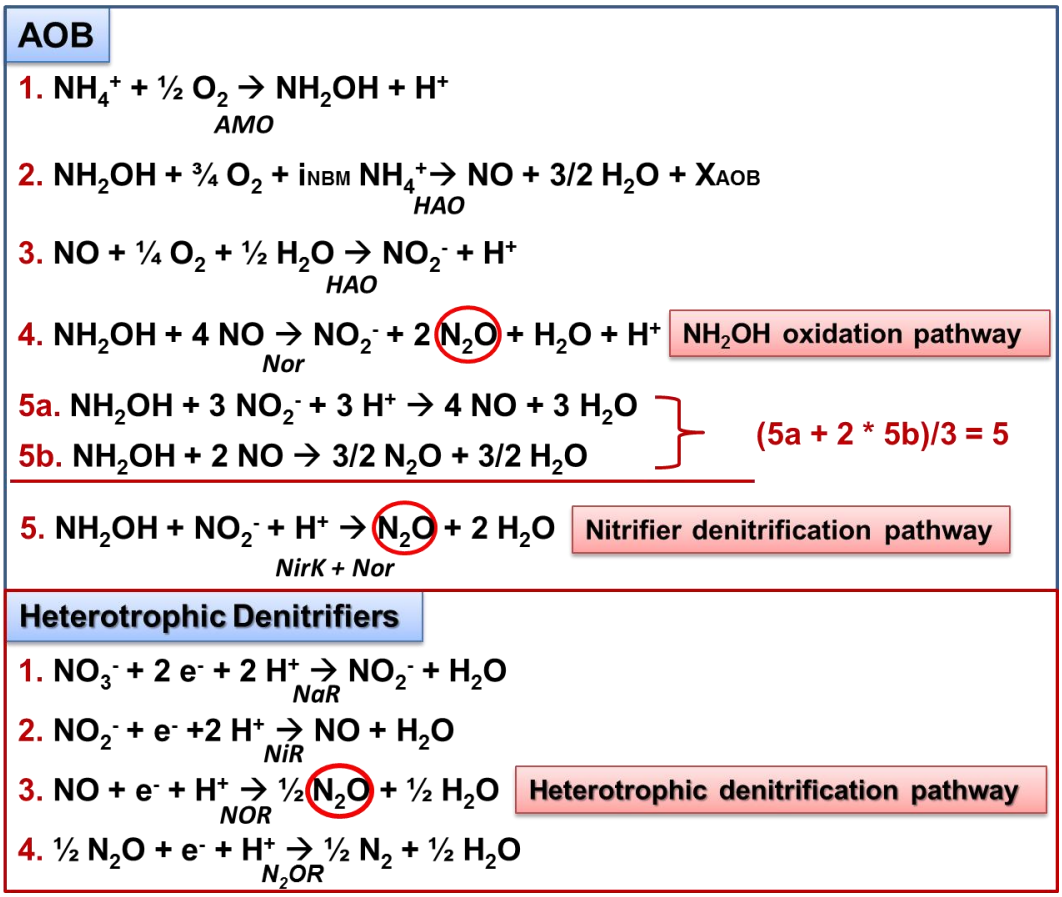

Figure 2. The three pathways for the N_2O production considered in our model: NH_2OH oxidation pathway (AOB pathway), nitrifier denitrification (AOB pathway) and heterotrophic denitrification. The assumptions concerning the AOB and heterotrophic denitrification-related reactions were made in accordance to what was reported by Pocquet et al. [17] and Ni and Yuan [9].

Considering the assumptions made by Pocquet et al. [17], our work included the following five AOB reactions (Fig. 2): (1) NH_4^+ oxidation to NH_2OH, (2) NH_2OH oxidation to nitric oxide (NO), (3) NO oxidation to NO_2^-, (4) NO reduction to N_2O along with the NH_2OH oxidation to NO_2^- (N_2O production via the NH_2OH oxidation pathway), (5) NO_2^- reduction combined with NH_2OH oxidation to produce N_2O (N_2O production by the nitrifier denitrification pathway,

combination of reactions 5a and 5b). The additional four reactions related to the heterotrophic denitrification pathway and the enzymes catalyzing all the steps of the three pathways are schematically shown in Fig. 2. The enzymes involved are: AMO (NH_4^+ monooxygenase), HAO (NH_2OH oxidoreductase), Nor (NO reductase), NirK (NO_2^- reductase) for the AOB, and NaR (NO_3^- reductase), NiR (NO_2^- reductase), NOR (NO reductase), and N_2OR (N_2O reductase) for the heterotrophs [9, 17]. Pocquet et al. [17] grouped together the NO_2^- reduction to NO (NirK enzyme) and the reduction of NO to N_2O (Nor enzyme) into one reaction: NO_2^- being directly reduced to N_2O (Fig. 2, eq. 5). They assumed that the Nor quickly consumed the NO produced by the aid of NirK or, equivalently, that the NO produced through the nitrifier denitrification pathway was converted to N_2O at a high rate. The latter was necessary in order to avoid a NO loop.

The model also considered P removal. Based on the ASM2d [29] structure, the following PAO-related processes were included: storage of polyhydroxyalkanoate (PHA), aerobic storage of polyphosphate (PP), aerobic growth of PAO and lysis of PHA, PP and PAO. Moreover, the anoxic processes of PP storage and PAO growth were expanded to cover all the four possible electron acceptors included in the current model: NO_3^-, NO_2^-, NO and N_2O, following the same reactions as those for the ordinary heterotrophs (Fig. 2).

The final model was developed in Matlab® using the *ode15s* function, which is a variable order method recommended for stiff systems. The settling was modeled with reference to the study by Takács et al. [30]. Steady-state was achieved by simulating the WWTP with constant influent composition for a period of 200 d.

All the kinetic parameter values were normalized for 20 ºC from the ASM2d section of Henze et al. [29]. The AOB decay and growth rates were taken from Hiatt and Grady [24]; μ_{AOB}=0.78 d^{-1}, b_{AOB}=0.096 d^{-1}. As far as the growth/decay rates for the nitrite oxidizing bacteria (NOB) are concerned, two different sets were tested for comparative purposes; the first from Hiatt and Grady [24] (μ_{NOB}=0.78 d^{-1}, b_{NOB}=0.096 d^{-1}), and the second one from Jubany et al. [31] (μ_{NOB}=1.02 d^{-1}, b_{NOB}=0.17 d^{-1}).

Tables presenting the stoichiometric/kinetic parameters, the stoichiometry, and the process rates of the processes integrated into our model are given in detail as Supportive Material.

2.3 N_2O emission factor (EF) modeling

The N_2O emission factor in our model was calculated in three ways: i) considering both the stripped N_2O and the N_2O in the effluent to reflect the most conservative estimation (N_2O-EF_{TOTAL}, Eq. 1.1), ii) considering only the stripping contribution (N_2O-EF_{GAS}, Eq. 1.2), and iii) considering only the effluent contribution (N_2O-EF_{EF}, Eq. 1.3).

$$\boldsymbol{N_2O\text{-}EF_{TOTAL}}(\%) = \mathbf{100} \cdot \frac{\boldsymbol{N_2O_{ST}+N_2O_{EF}}}{\boldsymbol{N_{IN}}} \quad \textbf{(Equation 1.1)}$$

$$\boldsymbol{N_2O\text{-}EF_{GAS}}\ (\%) = \mathbf{100} \cdot \frac{\boldsymbol{N_2O_{ST}}}{\boldsymbol{N_{IN}}} \quad \textbf{(Equation 1.2)}$$

$$\boldsymbol{N_2O\text{-}EF_{EF}}\ (\%) = \mathbf{100} \cdot \frac{\boldsymbol{N_2O_{EF}}}{\boldsymbol{N_{IN}}} \quad \textbf{(Equation 1.3)}$$

Where N_2O_{ST} is the amount of N_2O stripped from the aerobic reactor, N_2O_{EF} the N_2O in the effluent of the plant and N_{IN} the total N-content of the influent, which was calculated with Eq. 2.

$$N_{IN}\,(gN\cdot d^{-1}) = Q_{IN}\cdot(S_{NH4} + S_{NO3} + S_F\cdot i_{NS_F} + X_S\cdot i_{NX_S} + S_I\cdot i_{NS_I} + X_I\cdot i_{NX_I})$$

(Equation 2)

With Q_{IN} as the influent flowrate, and the rest of terms following the ASM2d nomenclature reported by Henze et al. [29]: S_{NH4}, S_{NO3}, S_F, X_S, S_I and X_I denote the influent concentrations for NH_4^+ (gNH_4^+-N m^{-3}), NO_3^- (gNO_3^--N m^{-3}), fermentable substrate (gCOD m^{-3}), slowly biodegradable substrate (gCOD m^{-3}), inert soluble substrate (gCOD m^{-3}) and inert particulate substrate (gCOD m^{-3}), respectively. i_{NS_F}, i_{NX_S}, i_{NS_I} and i_{NX_I} are the N-content (gN g^{-1}COD) of S_F, X_S, S_I and X_I, respectively.

The N_2O in the effluent (N_2O_{EF}) was calculated using the N_2O concentration (gN m^{-3}) in the aerobic reactor (N_2O_{AE}) as in Eq. 3:

$$N_2O_{EF}\,(gN\cdot d^{-1}) = Q_{IN}\cdot N_2O_{AE} \qquad \textbf{(Equation 3)}$$

Finally, the stripped N_2O (N_2O_{ST}) was calculated using Eq. 4, where k_La_{N2O} is the volumetric mass transfer coefficient for N_2O, V_{AE} is the volume of the aerobic reactor and the SE factor denotes 'stripping effectivity'. We applied SE values in the range 0-1 as a mechanism enabling us to investigate the impact of the non-ideality of this typical simplified modeling approach on the N_2O EF.

$$N_2O_{ST}\,(gN\cdot d^{-1}) = k_La_{N_2O}\cdot V_{AE}\cdot N_2O_{AE}\cdot SE \qquad \textbf{(Equation 4)}$$

The volumetric mass transfer coefficient (k_La) comprises the global transfer coefficient k_L along with the interfacial area a (interphase transport surface between liquid and gas per unit of reactor volume). The k_La_{N2O} resulted from Eq. 5 following Higbie's penetration model [32]:

$$\boldsymbol{k_L a_{N_2O}(d^{-1}) = k_L a_{O_2} \cdot \sqrt{\frac{Dif_{N2O}}{Dif_{O2}}}} \qquad \textbf{(Equation 5)}$$

$k_La_{O_2}$ is the volumetric mass transfer of oxygen in the aerobic reactor, which was automatically calculated by including the DO control system in the model. Dif_{N2O} is the molecular diffusivity of N_2O in water ($2.11 \cdot 10^{-9}$ m^2 s^{-1} at 20 ºC) and Dif_{O2} the molecular diffusivity of oxygen in water ($2.01 \cdot 10^{-9}$ m^2 s^{-1} at 20 ºC) [33].

2.4 Continuity check

The continuity of the model was verified to detect typos, inconsistencies, gaps or conceptual errors in the proposed extension following the methodology proposed by Hauduc et al. [34] who checked and corrected seven of the most commonly used ASM models. The method consists in the analysis of the matrix which results after multiplying the stoichiometric matrix (available in the Supportive Material section) and the composition matrix (i.e. conversion factors of each state variable to COD, N, P, charge and total suspended solids (TSS)). The tolerance allowing the acceptance of the continuity matrix was set at 10^{-15} as suggested by Hauduc et al. [34]. The stoichiometric matrix, the composition matrix (definitions and numerical values) and the continuity check can be found in the Supportive Material.

2.5 Sensitivity analysis (SA)

A local SA was conducted to establish the parameters that were more sensitive to $N_2O\text{-}EF_{TOTAL}$ (Eq. 1.1). Reichert and Vanrolleghem [35] defined the relative sensitivity ($S_{i,j}$) of an output (y_i) with respect to a parameter (θ_j) as in Eq. 6:

$$\mathbf{S_{i,j} = \frac{\theta_j}{y_i} \cdot \frac{\partial y_i}{\partial \theta_j}} \qquad \textbf{(Equation 6)}$$

In our case, the $N_2O\text{-}EF_{TOTAL}$ at steady state was used as the model output. The parameters involved in the SA were all the kinetic and stoichiometric parameters as well as the conversion factors that are given in the Supportive Material. However, the S_I production in hydrolysis (f_{SI}) and the P-content of S_I (i_{PSI}) were excepted since they were fixed at zero. Furthermore, the anoxic growth factor (n_G) parameter was adjusted to 0.9 (instead of 1) to compute the forward difference. The NOB growth and decay parameters were retrieved from the study by Hiatt and Grady [24]. A total number of 104 parameters were included in the SA.

The central difference method was used to calculate the sensitivity for each parameter. Different perturbation factors, ranging from 0.01% to 10%, were tested to ensure that the perturbation factor selection did not affect the parameter ranking.

As will be discussed in sections 3.1, 3.2 and 3.4, different DO values in the aerobic reactor (e.g. varying from 1 to 4 mg L^{-1}), resulted in very different EFs. Hence, the SA was performed under two different steady-state scenarios (i.e. at high and low DO setpoint in the aerobic reactor, set as equal to 3 and 1 mg L^{-1}, respectively). The latter was decided to better understand the causes of

high N_2O emission. During the SA tests, the influent S_{NH4} was fixed at 30 mg L^{-1} and the SE at 0.5.

3. Results and discussion

3.1 DO impact on nitrification and N_2O emissions

The model was applied to investigate the effect of DO concentration (from 0 to 4 mg L^{-1}) in the aerobic reactor on the nitrification process and, finally, on the N_2O emissions. The evolution of N_2O-EF_{TOTAL}, AOB and NOB activity and NH_4^+, NO_2^- and NO_3^- concentrations with respect to different DO levels are shown in Fig. 3.

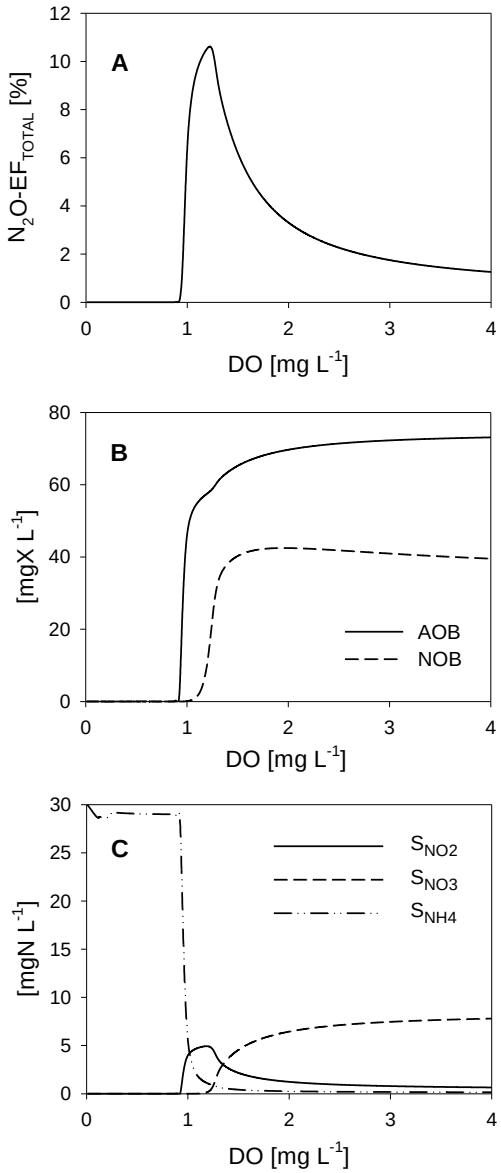

Figure 3. DO effect in the aerobic reactor on the steady state values of (A) N_2O emission factor, (B) AOB and NOB concentration, and (C) NO_2^-, NO_3^- and NH_4^+, concentration. The SE was 1 and both the AOB and NOB growth and decay parameters were taken from the study by Hiatt and Grady [24].

Fig. 3B and 3C show that neither AOB/NOB growth nor NO_2^-/NO_3^- production was observed under oxygen-limiting conditions (i.e. for DO values lower than approximately 0.8 mg L^{-1}). The NH_4^+ concentration increased compared to the respective influent one (S_{NH4}=20 mgN L^{-1}) because of hydrolysis processes releasing NH_4^+ and no nitrification happening due to the low DO. The DO increase from 0.8 mg L^{-1} onwards enhanced the AOB growth. On the contrary, the NOB growth only commenced at a DO around 1.1 mg L^{-1} (Fig. 3B). These threshold values (i.e. 0.8 and 1.1 mg L^{-1}) are mainly determined by the oxygen affinity constants values and, thus, from mass transfer and operational conditions. The NOB have a lower affinity to oxygen compared to the AOB [36], which explains why synergies that result in partial nitrification/nitritation (i.e. NH_4^+ oxidation to NO_2^-) are based on the selection of a proper DO setpoint [37]. In accordance to this, our simulation results demonstrated that the AOB prevailed over the NOB under relatively low DO levels (i.e. DO between 0.8 and 1.1 mg L^{-1}) (Fig. 3B). In this range, the NH_4^+ concentration decreased, while NO_2^- started increasing; nitritation resulted in NO_2^- accumulation (Fig. 3C). Within the same DO range (0.8-1.1 mg L^{-1}), we observed a significant N_2O emission factor increase up to almost 10.5% (Fig. 3A). In this case, the dominant N_2O production pathway was nitrifier denitrification; under such oxygen-limiting conditions, NO_2^- substitutes oxygen at the role of the final electron acceptor and, thus, the AOB perform nitrifier denitrification [11, 38-39]. Our observations agree with previous studies investigating the preferred N_2O production pathway at different DO levels. For example, Law et al. [40] worked with an enriched AOB culture in a lab-scale nitritation system fed with anaerobic digester liquor; amongst the two AOB pathways, nitrifier denitrification was suggested as predominant at the lowest DO values tested (i.e. 0.55 and 1.3 mg L^{-1}; the highest tested was 2.3 mg L^{-1}) and decreased NO_2^- concentrations. Similarly, the DO effect on N_2O production by an

enriched nitrifying sludge was investigated in a lab-scale sequencing batch reactor (SBR); the DO increase from 0.2 to 3 mg L^{-1} was correlated with a decreased contribution of the nitrifier denitrification pathway [41].

Our simulations showed that, as soon as DO reached the level of 1.5 mg L^{-1}, AOB and NOB were stabilized around 70 mg L^{-1} and 40 mg L^{-1}, respectively (Fig. 3B). Complete nitrification started and resulted in less NO_2^- accumulation as well as in the gradual nitrifier denitrification pathway deactivation. This is depicted in Fig. 3A through a continuous N_2O-EF_{TOTAL} decrease that initiated at a DO around 1.5 mg L^{-1} and was reinforced with the further DO increase. Furthermore, NO_3^- production began; the latter indicating that full nitrification was happening (Fig. 3C). At high DO levels (i.e. >3 mg L^{-1}), the N_2O emission factor was significantly lower; less than 2%. In terms of N_2O emission mitigation, high DO (i.e. >3 mg L^{-1}) proved to be beneficial. However, it is an energy-consuming option. For instance, a study on a plug-flow (three-pass) full-scale municipal WWTP in the UK indicated that N_2O emissions added 13% to the carbon footprint of the plant because of the electricity needed to run the nitrifying process [42]. Intermittent aeration regimes can be applied as a promising option to reduce aeration costs by 33-45%. However, this strategy is likely to disturb the bioreactor operation, hinder the nitrifying population activity, and, hence, create conditions favouring the N_2O generation. Consequently, an additional carbon footprint related to the N_2O emissions can arise [43]. Therefore, it is essential to consider the potential magnitude of N_2O process emissions before adopting low-energy strategies [42]. Increased N_2O production and emission is probable under low-DO conditions suggesting a high final overall carbon footprint for a WWTP. It is useful to investigate multiple DO values to find an interval inside which neither the nitrification process

nor the plant's carbon footprint is compromised; this can be between 1.8 and 2.5 mg L^{-1} for our study.

3.2 Influence of two different parameter sets for the NOB growth and decay on the N_2O emission factor (EF)

As explained in section 2.2, two different sets regarding the growth/decay rates for the NOB were tested for comparative purposes; one from Hiatt and Grady [24] (μ_{NOB}=0.78 d^{-1}, b_{NOB}=0.096 d^{-1}) and the second one from Jubany et al. [31] (μ_{NOB}=1.02 d^{-1}, b_{NOB}=0.17 d^{-1}).

Short-cut biological nitrogen removal, i.e. nitritation (NH_4^+ oxidation to NO_2^-) followed by denitritation (NO_2^- reduction to N_2) emerged as extremely interesting in the domain of wastewater treatment, especially in the cases of wastewaters with high NH_4^+ content [44]. Compared to full nitrification (i.e. NH_4^+ oxidation to NO_3^-), the short-cut process has proved to be more advantageous in terms of COD demand (40% reduction during denitrification) and denitrification rate (63% higher) [45]. Furthermore, it can induce a 25% decrease in the oxygen demand during nitrification because of the avoidance of nitratation (i.e. NO_2^- oxidation to NO_3^-) [46]. If nitritation is the target for the plant operators, it is essential to apply conditions which favour the AOB activity but suppress the NOB community. The relative influential parameters include temperature, pH and DO [44]. The current study focused on the DO effect; temperature and pH were considered stable for all simulations (T=20 ºC and pH=7). Low-DO environments are expected to enhance the NO_2^- accumulation [47-49].

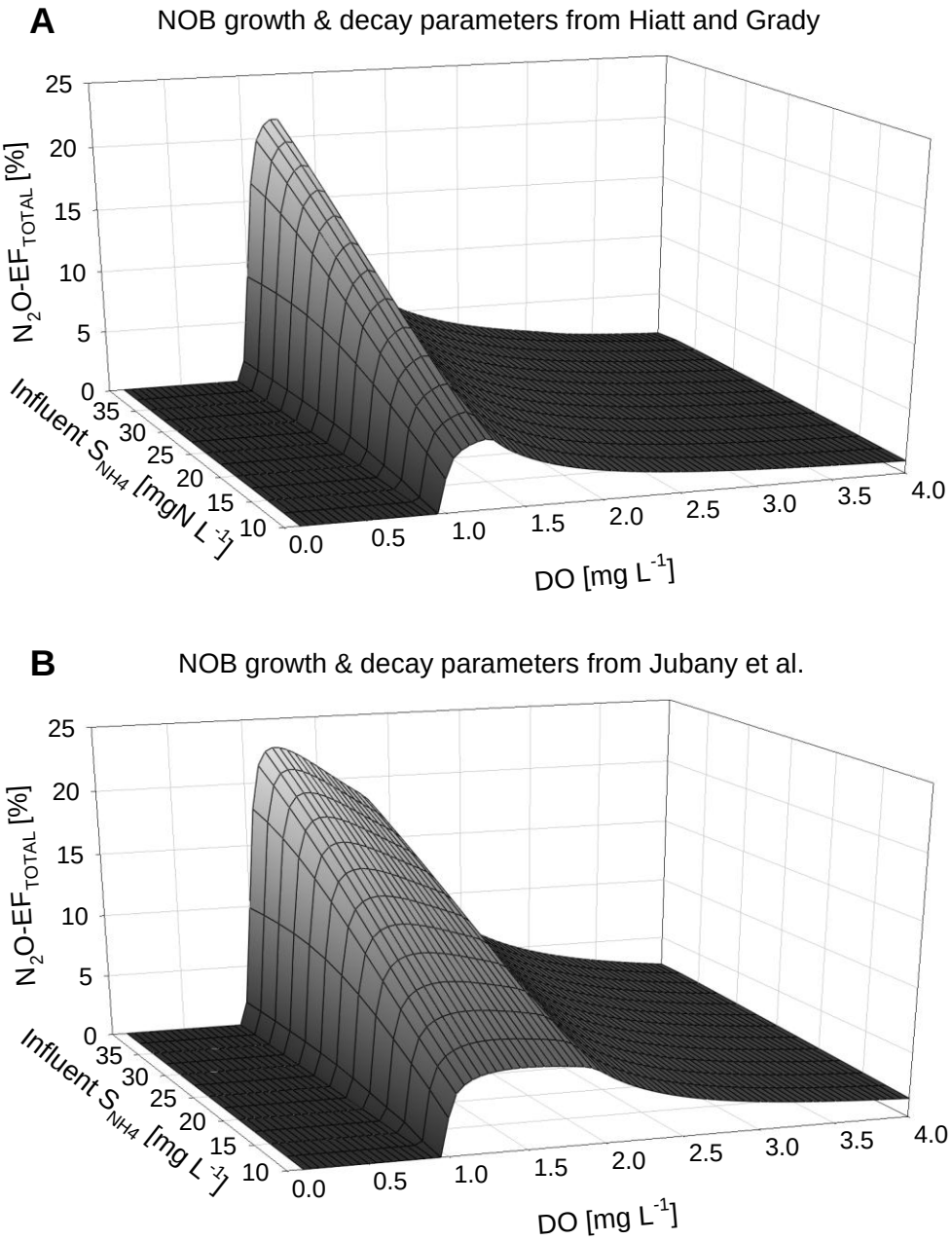

Figure 4. The steady-state N_2O emission factor with respect to different DO setpoints in the aerobic reactor (0 to 4 mg L^{-1}) and influent S_{NH4} concentrations (10 to 40 mg L^{-1}). The selected SE was 1. A) NOB parameters of Hiatt and Grady [24]. B) NOB parameters of Jubany et al. [31].

Fig. 4 shows the effect on N_2O-EF_{TOTAL} in different scenarios with the DO concentration ranging from 0 to 4 mg L^{-1} and the influent S_{NH4} from 10 to 40 mg L^{-1}. For this part of the simulations, we used the maximum theoretical stripping efficiency (SE=1). The latter offered the possibility to examine a range of DO and influent NH_4^+ values which embodied the worst-case scenario (i.e. highest N_2O emissions). The simulations were executed for each one of the different parameter sets for the NOB growth and decay. In both cases, the general trends were similar. First, no nitrification and, subsequently, no N_2O emission was noticed at very low DO (i.e. below 0.8 mg L^{-1}). The DO increase provided the conditions for the initiation of nitritation. The highest N_2O emissions occurred for (still relatively low) DO levels between 0.8 and 1.8 mg L^{-1}; it is when nitritation led to NO_2^- accumulation and, afterwards, to N_2O production through the nitrifier denitrification pathway. The model predicted the highest N_2O emission (around 22%) under the following combination: DO around 1.1 mg L^{-1}, influent N-NH_4^+=40 mg L^{-1} (i.e. the highest tested) and SE=1. The further DO increase above 1.8 mg L^{-1} resulted in the significant N_2O-EF_{TOTAL} decrease (reaching almost 2% after DO>2.5 mg L^{-1}), as a consequence of the NO_2^- consumption through full nitrification. Similar results have been reported in past experimental studies. Pijuan et al. [50] monitored the nitritation process in an airlift system with granular biomass to explore the DO effect. N_2O emissions decreased from 6% to 2.2% of N-oxidized when DO increased from 1 to 4.5 mg L^{-1}. Moreover, Rathnayake et al. [51] observed that the N_2O emissions over the oxidized NH_4^+ decreased from 2.9% (DO=0.6 mg L^1) to 1.4% (DO=2.3 mg L^1) in a lab-scale nitritation reactor fed with synthetic wastewater.

Furthermore, according to the trends noted while examining the N_2O-EF_{TOTAL} versus the influent S_{NH4} concentration, the N_2O emissions increased with the increase of the influent NH_4^+ load. As a result, lower loaded influents are expected to have lower emissions. While investigating the

combined effect of N-loading rate and DO in a pilot-scale SBR treating reject water, Frison et al. [52] tested two different combinations of these parameters (first combination: volumetric N-loading rate=1.08 kg N m^{-3} d^{-1} & DO=0.95 mg L^{-1}; second combination: volumetric N-loading rate=0.81 kg N m^{-3} d^{-1} & DO=1.48 mg L^{-1}). N_2O emissions decreased from 1.49% to 0.24% of the influent N-load when switching from the first to the second combination. The higher DO along with an influent N-loading not exceeding the system's capacity resulted in lower NO_2^- accumulation and N_2O emissions. Similarly, our model predicted the increase in N_2O emissions after applying higher S_{NH4} influent concentrations along with lower DO.

However, it is noted that the N-removal via NO_2^- was prolonged with the NOB growth and decay parameters from Jubany et al. [31]. Nitritation occurred at around 0.8<DO<1.8 mg L^{-1} with the parameters from Hiatt and Grady [24], whereas at around 0.8<DO<2.2 mg L^{-1} with the parameters from Jubany et al. [31] (Fig. 4). The NOB growth and decay rates of Jubany et al. [31] are 23.5% and 43.5% higher, respectively, than the ones of Hiatt and Grady [24]. However, the most important parameter affecting the N-removal via NO_2^- is the NOB-related half-saturation coefficient for oxygen. This parameter was 1.2 mg L^{-1} for Hiatt and Grady [24], whereas equal to 1.75 mg L^{-1} [44, 48] for Jubany et al. [31]. This higher value increases the range of DO values leading to a limitation of NOB activity, and hence provokes a higher operational region with important N_2O emission.

Finally, the results obtained in this section match with past experimental observations according to which the operational parameters mostly contributing to the N_2O generation are linked to insufficient DO levels at the nitrification stage and increased NO_2^- concentration during both nitrification and denitrification [10-12].

3.3 Effect of the stripping effectivity (SE) on the N_2O emission factor (EF)

Even though N_2O is an intermediate of heterotrophic denitrification, aerobic (nitrification-related) compartments in WWTPs are the major N_2O emission hotspots. Stripping occurs during aeration and the produced N_2O is emitted into the atmosphere [13, 53].

As mentioned in section 2.3, our modeling concerning the N_2O stripping was based on the k_La approach. Moreover, it was enriched by the SE which acted as a coefficient describing the divergence of the model prediction (Eq. 4) with respect to ideality (SE=1). Eq. 4 simplifies the real stripping process by assuming the following: i) the air bubbles are always free of N_2O; their enrichment in N_2O is negligible as they rise up in the basin, ii) the liquid phase (as DO or N_2O concentration) has a homogeneous composition, and iii) the same k_La independently of the liquid depth. The combined effect of different DO levels and the highest influent S_{NH4} value tested (i.e. 40 mg L^{-1}) on the N_2O-EF under different SEs (i.e. 0, 0.1, 0.25, 0.5, 0.75, 1) was evaluated using the parameters by Hiatt and Grady [24]. It is presented in Fig. 5 for N_2O-EF_{TOTAL} (i.e. considering both the N_2O stripped and the N_2O contained in the effluent) as well as for the N_2O-EF_{GAS} (referring exclusively to the stripping contribution).

Under the application of the highest influent S_{NH4} value tested in this study (i.e. 40 mg L^{-1}), the trends were always similar and the maximum N_2O-EF was always observed for a DO around 1.2 mg L^{-1}. However, the maximum absolute values differed. In specific, the maximum N_2O-EF_{GAS} values ranged from 0% (SE=0) to ~21.1% (SE=1), while the maximum N_2O-EF_{TOTAL} values were between 6.3% (SE=0) and ~22% (SE=1). In other words, the SE increase led to a general rise in the EF. This was sharper in the beginning (SE: 0→0.1) and, then, more gradual (SE: 0.25→1) (Fig. 5). The observed trend reflects that a lower SE gives more chances for N_2O to

follow the denitrification pathway (reaction 4 of denitrification in Fig. 2), thus favouring its consumption instead of its stripping.

For each of the SE values tested, the N_2O-EF_{TOTAL} was always higher than the respective N_2O-EF_{GAS} one, but not significantly (Fig. 5). The latter showed that the N_2O stripping majorly contributed to the N_2O EF estimation. Only in the case of SE=0 (the hypothetical case of no stripping) the contribution of the dissolved N_2O was very significant. More importantly, our results indicated that the SE factor was a very significant contributor to the final EF results. Hence, a more detailed modeling of the stripping process in the future, avoiding the simplifications previously commented can potentially increase the accuracy in the EF prediction and prevent its overestimation.

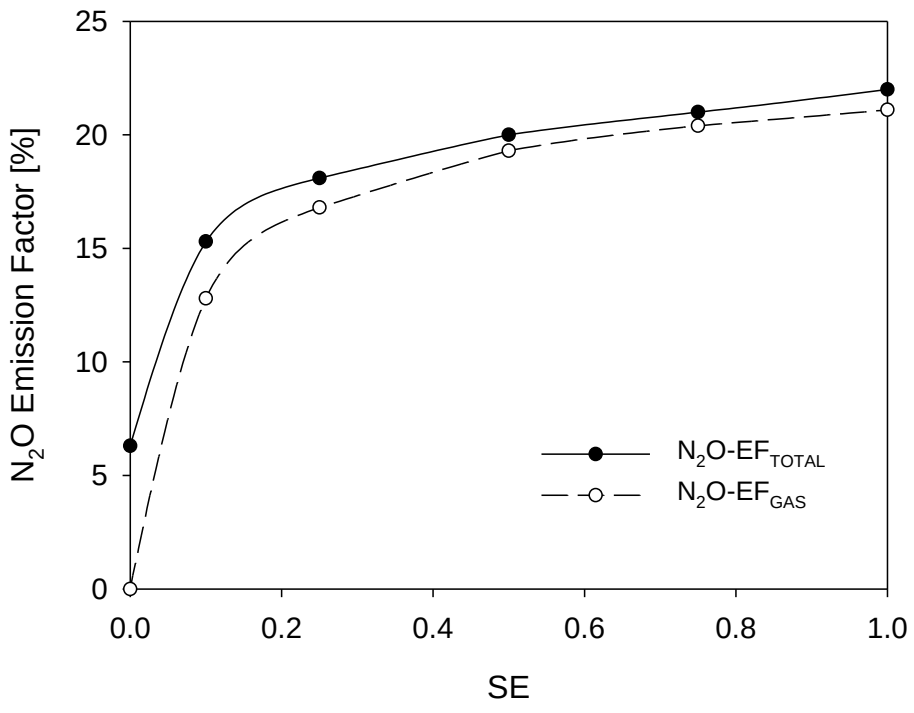

Figure 5. The maximum N_2O emission factor (N_2O-EF_{TOTAL} considering both the N_2O stripped and the N_2O contained in the effluent; N_2O-EF_{GAS} referring exclusively to the contribution of the N_2O stripping) observed for the different SE values (0, 0.1, 0.25, 0.5, 0.75, 1) tested during our simulations. The influent S_{NH4} value was considered equal to 40 mg L^{-1} and the parameters were retrieved from the study by Hiatt and Grady [24].

3.4 Modeling of dynamic N_2O emissions under disturbances

An additional goal of this work was to examine how the N_2O emissions were influenced by influent disturbances under different DO scenarios. Transition states after a disturbance are the most favourable scenarios for intermediates accumulation and, thus, higher N_2O emissions. As an example, the effect of a S_{NH4} concentration increase in the influent was studied (as a 'step' increase from 20 to 30 mgN L^{-1} on the 10th day of the plant operation). This was examined for various scenarios with different combinations of SE and DO control values in the aerobic reactor.

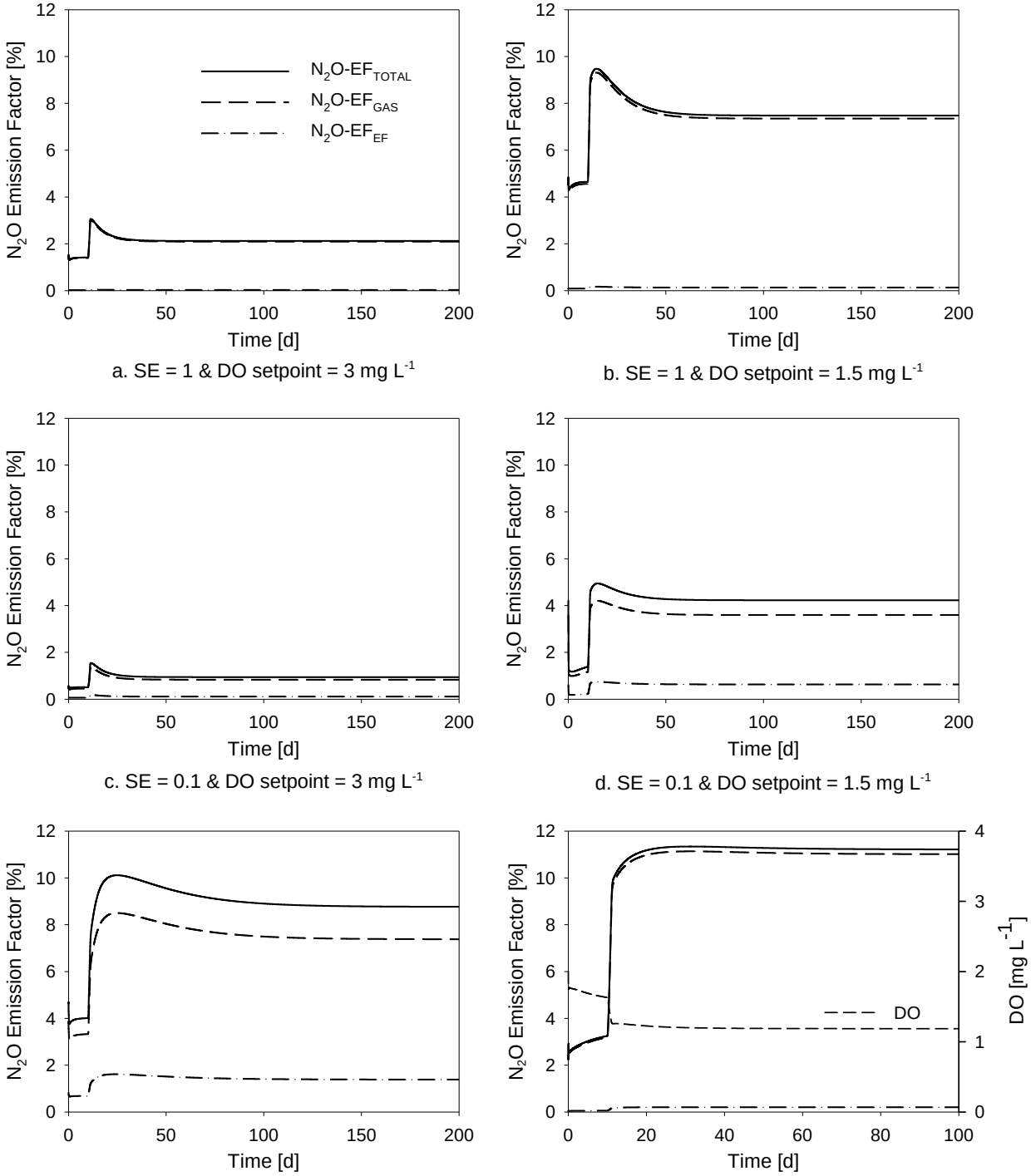

a. SE = 1 & DO setpoint = 3 mg L^{-1}

b. SE = 1 & DO setpoint = 1.5 mg L^{-1}

c. SE = 0.1 & DO setpoint = 3 mg L^{-1}

d. SE = 0.1 & DO setpoint = 1.5 mg L^{-1}

e. SE = 0.1 & DO setpoint = 1.2 mg L^{-1}

f. SE = 1 & no DO control

Figure 6. The effect of increasing the influent S_{NH4} concentration (from 20 to 30 mgN L^{-1}) at the 10th day of the plant operation on the N_2O-EF. Different SE values (1 and 0.1) and DO setpoints (3 mg L^{-1}, 1.5 mg L^{-1}, 1.2 mg L^{-1} and no DO control) were tested.

For the scenarios a and b, the SE was 1 to enable the observance of the full stripping effect under the sudden change of the operational conditions. The fast S_{NH4} increase resulted in a rapid increase of N_2O emissions. The N_2O-EF_{TOTAL} presented the following trends: 1.4→3.1% almost up to the 12th day of operation (scenario a) and 4.5→9.6% until the 17th day (scenario b). Then, a gradual EF reduction started until it was stabilized at lower levels: at ~2.1% after the 30th day (scenario a), and at ~7.5% after the 40th day (scenario b) (Fig. 6). The DO control setpoint in case b was significantly lower than in scenario a; thus, higher absolute EF values were expected as previously seen in Fig. 4A. Under such conditions, the AOB bacteria are known to induce nitritation, use NO_2^- as terminal electron acceptor and, finally, produce N_2O (nitrifier denitrification pathway) [54-56]. Indeed, low DO (e.g. <1.5 mg L^{-1}) has been experimentally connected with the achievement of nitritation, the subsequent NO_2^- accumulation and NOB washout [57-60]. For both scenarios a and b, the downward trend of the N_2O-EF indicated that NOB were growing and performing NO_2^- oxidation. However, the fact that the final N_2O-EF never recovered its initial value implies that the NOB growth only covered part of the new NO_2^- oxidation requirements. Fig. 7 shows the effect of scenarios a and b on the AOB and NOB growth. In both cases, the AOB growth was always sharper than the respective NOB one after the operational change on the 10th day. In accordance to what is seen in Fig. 7, the AOB population has been reported to prevail over the NOB under increased NH_4^+ availability and controlled aeration [61].

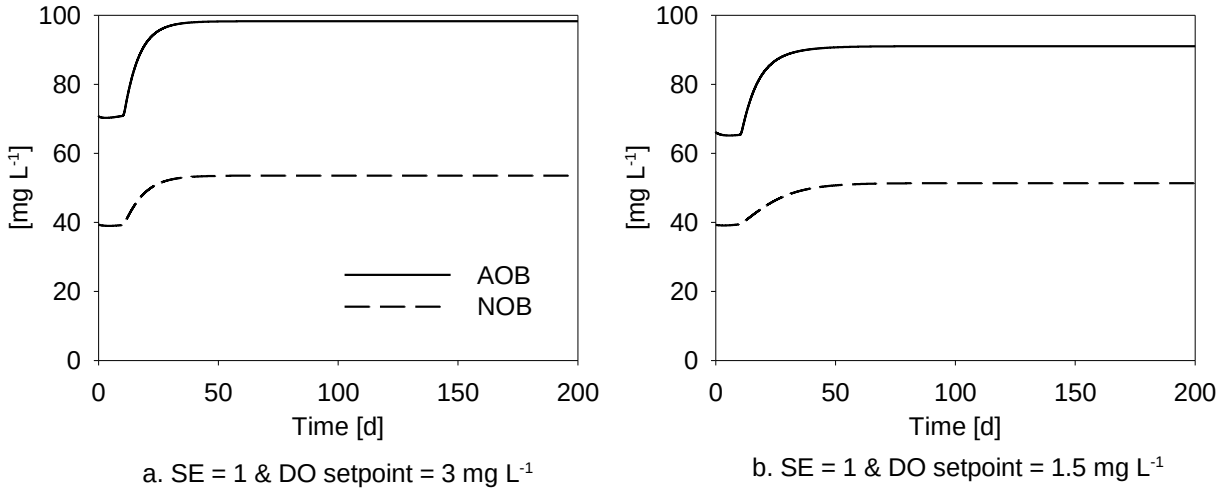

Figure 7. The AOB and NOB evolution after increasing the influent S_{NH4} concentration (from 20 to 30 mgN L^{-1}) on the 10th day of the plant operation. Different DO control setpoints (3 mg L^{-1} and 1.5 mg L^{-1}) were compared for a SE=1.

For the same DO levels, different SE values were tested to simulate the full and reduced stripping effect via fixing the SE as equal to 1 and 0.1, respectively (comparison between scenarios a and c, and comparison between scenarios b and d in Fig. 6). In terms of N_2O-EF_{TOTAL}, the same trends were observed: a fast increase followed by a decrease with a final value stabilized higher than the one observed before the S_{NH4} increase. The SE decrease (from 1 to 0.1) explains the increased distance between the lines of N_2O-EF_{TOTAL} and N_2O-EF_{GAS}. The emissions were lower in the SE=0.1 cases (Fig. 6c and 6d) and more N_2O was considered as remaining dissolved, thus coming out in the effluent. A lower SE value (i.e. 0.1) imposes less stripping to the system, which results in: i) an increased N_2O concentration in the aerobic reactor, and ii) an increased recycling of N_2O to the anoxic reactor leading to higher N_2O consumption.

Scenario e studies the effect of working at the DO setpoint of 1.2 mg·L^{-1} and SE =0.1, in order to show clearly the effect of working under DO conditions unfavorable to the NOB growth. N_2O emissions higher than 9% were observed because of N-removal via NO_2^- and NOB washout, as detailed in sections 3.1 and 3.2.

However, all the scenarios previously commented (i.e. scenarios a - e) were DO-controlled; this enabled simulating how increasing aeration by the control loop allowed the maintenance of the desired DO concentration. Scenario f, though, showed that the effect of the S_{NH4} influent increase can be higher and more persistent in a non-DO-controlled environment. The increase of NH_4^+ load decreases the DO concentration, and can move the system from an operational point with full nitrification to a point with N-removal via NO_2^- which explains the higher EF noted.

A sudden operational change imposed to the system such as the one examined in this section (i.e. a step increase in the influent S_{NH4} from 20 to 30 mg L^{-1}) increased the N_2O emissions. The AOB and NOB populations were affected, with the AOB growth being quicker and higher compared to the respective NOB one. Thus, N-removal via NO_2^- was increased and N_2O was produced through nitrifier denitrification. The magnitude of the emissions depended on the imposed SE value and DO control setpoint; the higher the imposed SE value, the higher the stripping effect and, thus, the anticipated emissions. Moreover, a lower DO setpoint placed the system under nitritation regime, thus creating the conditions for the activation of the nitrifier denitrification pathway. Under no DO control, the environment within the reactor became even more favorable to N-removal via NO_2^-, hence greatly increasing the EF.

3.5 Sensitivity Analysis (SA) of the developed model

Table 2 shows the 40 most sensitive parameters to the N_2O-EF_{TOTAL} for the two studied scenarios with influent S_{NH4}=30 mg L^{-1} and SE=0.5 (first: DO in the aerobic reactor=3 mg L^{-1}; second: DO in the aerobic reactor=1 mg L^{-1}). The values are listed in descending order considering the $S_{i,j}$ absolute values calculated with Eq. 6. The sign of the sensitivity indices is maintained since it contains information: a positive sensitivity index indicates that an increase in the parameter results in an increase of the N_2O-EF_{TOTAL}, while a negative sensitivity suggests that an increase in the parameter will lead to a decrease in the N_2O-EF_{TOTAL}. The results showed in Table 2 were obtained with a perturbation factor of 0.01%. The choice on the perturbation factor was based on the work by De Pauw [62] who suggested to use a factor producing equal derivative values for forward and backward differences. Nevertheless, the perturbation factor did not significantly affect the parameter categorization (data not shown).

Table 2. Sensitivity analysis results for the two different operational modes (first: DO_{AE} =3 mg L^{-1}; second: DO_{AE} =1 mg L^{-1}); both with influent S_{NH4}=30 mg L^{-1} and SE=0.5. DO_{AE} stands for the DO control setpoint in the aerobic reactor.

Order	**DO_{AE}=3 mg L^{-1}**		**DO_{AE}=1 mg L^{-1}**	
	Parameter	**Si,j**	**Parameter**	**Si,j**
1	μ_{NOB}	-2.138	Y_{AOB}	2.233
2	η_G	1.489	η_G	1.978
3	b_{NOB}	1.059	q_{AOB_AMO}	1.407
4	$q_{AOB\_N2O\_ND}$	0.997	Y_{PAO}	1.108
5	μ_{AOB_HAO}	-0.926	b_{AOB}	-1.024
6	$K_{I\_O2\_AOB}$	0.878	η_{G5}	-0.947
7	Y_{AOB}	0.863	K_{OH5}	-0.853
8	K_{HNO2_AOB}	-0.857	$q_{AOB\_N2O\_ND}$	0.841
9	K_{NO2_NOB}	0.851	K_{O2_AOB1}	-0.738

Order	DO_{AE}=3 mg L^{-1}		DO_{AE}=1 mg L^{-1}	
	Parameter	**Si,j**	**Parameter**	**Si,j**
10	Y_{PAO}	0.739	i_{NXS}	0.674
11	K_{O2_NOB}	0.629	Y_H	-0.470
12	η_{G5}	-0.620	Y_{PO4}	-0.435
13	K_{OH5}	-0.470	q_{PP}	0.400
14	K_{N2O_Den}	0.435	μ_{PAO}	-0.386
15	i_{NXS}	0.428	i_{NBM}	-0.375
16	b_{PAO}	-0.408	K_{HNO2_AOB}	-0.360
17	SE	0.375	i_{NSF}	0.338
18	Y_H	-0.364	$K_{I\_O2\_AOB}$	0.299
19	K_{MAX_P}	0.259	K_{MAX_P}	0.292
20	i_{NBM}	-0.247	SE	0.223
21	μ_{PAO}	0.246	K_{NH2OH_AOB}	-0.209
22	i_{NSF}	0.207	$K_{O2\_AOB\_ND}$	0.198
23	$K_{O2\_AOB\_ND}$	0.192	μ_{AOB_HAO}	-0.175
24	D_{O2}	-0.187	K_{N2O_Den}	0.170
25	D_{N2O}	-0.187	K_{S5}	0.166
26	K_{P_P}	-0.169	K_F	-0.157
27	K_{O2_AOB2}	0.167	Y_{PHA}	-0.149
28	K_{S5}	0.151	K_{NH4_AOB}	-0.137
29	b_H	0.149	n_{fe_H}	-0.134
30	Y_{PO4}	-0.135	K_{O2_P}	-0.132
31	K_{P_NOB}	0.122	b_H	0.121
32	q_{AOB_AMO}	-0.120	D_{O2}	-0.111
33	q_{PHA}	0.118	D_{N2O}	-0.111
34	K_H	-0.101	b_{PAO}	-0.101
35	K_F	-0.099	K_H	-0.098
36	n_{fe_H}	-0.094	k_La	0.089
37	Y_{PHA}	-0.094	K_{O2_AOB2}	0.082
38	q_{PP}	0.085	K_{IPP_P}	-0.074
39	η_{G3}	0.077	i_{PXS}	-0.073
40	i_{PXS}	-0.064	b_{PP}	-0.071

Different parameter ranking was found between the two scenarios: the most sensitive parameters to the N_2O-EF_{TOTAL} factor varied under the different DO setpoints. For the DO setpoint of 3 mg L^{-1}, the most sensitive parameters were those related to NOB metabolism, followed by those

related to the AOB activity and, finally, by those connected to PAO. The sensitivity of parameters referring to the NOB metabolism is important to understand potential NO_2^- accumulation. The latter will inevitably lead to changes in the total N_2O emission factor through the activation/deactivation of the nitrifier denitrification pathway, as discussed in section 3.1. On the other hand, under the DO setpoint of 1 mg L^{-1}, the AOB-related parameters were the most sensitive since limited NOB growth is anticipated in a low-DO environment (Fig. 3B). Hence, the NOB-related parameters became insensitive. For this scenario, the WWTP model operates under nitritation and increased N_2O production through nitrifier denitrification is expected (section 3.1).

For both tested scenarios, the anoxic growth factor (η_G) (i.e. the stoichiometric factor implicated in the growth of heterotrophs and PAO under anoxic conditions) had a severe impact on the N_2O emission factor. Considering that this parameter affects all the anoxic processes, its perturbation will change the stoichiometry of various processes.

It is worth mentioning that the SE only appears in the middle range of the table (17th and 20th for a DO setpoint of 3 and 1 mg L^{-1}, respectively). The reference value of this parameter (0.5) is essential to understand the sensitivity results. According to Fig. 5, the SE parameter has a significant effect on the $N_2O\text{-}EF_{TOTAL}$ while increasing from 0 to 0.2; its further increase from 0.2 to 1 has a lesser influence on the N_2O-EF values. Had this parameter been set at a lower value, its relative sensitivity would have increased.

Moreover, the conversion factors mostly affecting the $N_2O\text{-}EF_{TOTAL}$ were those related to the N-content (i_{NXS}, i_{NSF}) of state variables X_S and S_F. The latter can be justified by their interference in the calculation of the N_{IN} content (Eq. 2) and their subsequent effect on the $N_2O\text{-}EF_{TOTAL}$ estimation (Eq. 1.1).

Finally, we examined Table 2 again to see if any common parameters appeared in the first ten places for both scenarios. It was noted that n_G, $q_{AOB\_N2O\_ND}$ (maximum N_2O production rate by the nitrifier denitrification pathway), Y_{PAO} (yield coefficient for the PAO) and Y_H (yield coefficient for the heterotrophs) were amongst the first ten parameters for both DO setpoints; all with positive sensitivity. Hence, it can be deduced that decreasing these values leads to a decrease in the N_2O-EF_{TOTAL}. The n_G, Y_{PAO} and Y_H stoichiometric parameters, in specific, are included in the stoichiometry of the processes referring to the anoxic growth of PAO and heterotrophs. These processes can indeed be considered as significantly influencing the EF since they occur in an anoxic environment where N_2O can be consumed through denitrification. These results also show that the inclusion of PAO in our model has a significant impact in the EF related to the denitrification of N_2O. Lastly, the impact of the $q_{AOB\_N2O\_ND}$ kinetic parameter proved to be important in both scenarios. Given that $q_{AOB\_N2O\_ND}$ expresses the N_2O production rate through nitrifier denitrification, this observation indicates that nitrifier denitrification is probably the most important pathway to consider for the N_2O mitigation.

4. Conclusions

In this work, an ASM2d-N_2O model including COD, N and P removal along with all the known N_2O microbial pathways was developed for a municipal A^2/O WWTP, which can be highly useful for the estimation of the N_2O-EF. The following major conclusions were reached:

- Plant operators often opt for lower aeration to decrease a WWTP's energy requirements. With the aerobic DO ranging from 0.8 to 1.8 mg L^{-1}, the AOB prevailed over the NOB, thus promoting the shift from full to partial nitrification and, subsequently, the N_2O

production through nitrifier denitrification. Due to the important N_2O GWP, this operational change can result in a high final overall WWTP carbon footprint. Consequently, low aeration is desired only if it does not disturb the nitrification process.

- A SE coefficient (from 0 to 1) was added to reflect the non-ideality of the stripping modeling. Decreasing the SE was translated into higher N_2O concentration in the mixed liquor; the latter led to a higher N_2O denitrification rate and lower emissions.
- The effect of a sudden increase in the influent S_{NH4} from 20 to 30 mg L^{-1} was simulated. The AOB predominance over the NOB enabled NO_2^- accumulation and increased the nitrifier denitrification pathway. Higher emissions were observed under the following conditions: lower DO setpoints that created an environment more advantageous to nitrifier denitrification combined with higher SE values that raised the significance of the stripping effect.
- The sensitivity analysis showed that the NOB-related parameters had minor influence over the N_2O-EF under low-DO conditions, given the limited NOB growth at low DO. However, they were very significant at high DO due to its effect on the NO_2^- oxidation rate. The parameters n_G, $q_{AOB\_N2O\_ND}$, Y_{PAO} and Y_H were amongst the top ten for both DO setpoints tested. n_G, Y_{PAO} and Y_H are related to the N_2O consumption through denitrification. $q_{AOB\_N2O\_ND}$ indicates that nitrifier denitrification is probably the most important pathway to consider for the N_2O mitigation.

Acknowledgments

This project has received funding from the European Union's Horizon 2020 research and innovation program under the Marie Skłodowska-Curie C-FOOT-CTRL project (grant agreement No 645769). T.M. Massara is also grateful to the Natural Environment Research Council (NERC) of the UK for the 4-year full PhD studentship. B. Solís also acknowledges the support of Universitat Autònoma de Barcelona with a PIF pre-doctoral grant. J.A. Baeza, A. Guisasola and B. Solís are members of the GENOCOV research group (*Grup de Recerca Consolidat de la Generalitat de Catalunya*, 2014 SGR 1255).

References

[1] IPCC, Climate change 2013: the physical science basis. Contribution of Working Group I to the Fifth Assessment Report of the Intergovernmental Panel on Climate Change, in: T.F. Stocker, D. Qin, G.K. Plattner, M. Tignor, S.K. Allen, J. Boschung, A. Nauels, Y. Xia, V. Bex, P.M. Midgley (Eds.), Cambridge University Press, Cambridge and New York, 2013, pp. 1535.

[2] A.R. Ravishankara, J.S. Daniel, R.W. Portmann, Nitrous Oxide (N_2O): The Dominant Ozone-Depleting Substance Emitted in the 21st Century, Science 326 (2009) 123 LP-125. http://science.sciencemag.org/content/326/5949/123.abstract.

[3] J.H. Ahn, S. Kim, H. Park, B. Rahm, K. Pagilla, K. Chandran, N_2O emissions from activated sludge processes, 2008-2009: results of a national monitoring survey in the United States., Environ. Sci. Technol. 44 (2010) 4505–4511. doi:10.1021/es903845y.

[4] J. Foley, D. de Haas, Z. Yuan, P. Lant, Nitrous oxide generation in full-scale biological nutrient removal wastewater treatment plants, Water Res. 44 (2010) 831-844. doi:10.1016/j.watres.2009.10.033.

[5] A. Rodríguez-Caballero, I. Aymerich, R. Marques, M. Poch, M. Pijuan, Minimizing N_2O emissions and carbon footprint on a full-scale activated sludge sequencing batch reactor, Water Res. 71 (2015) 1-10. doi:10.1016/j.watres.2014.12.032.

[6] M.R.J. Daelman, B. De Baets, M.C.M. van Loosdrecht, E.I.P. Volcke, Influence of sampling strategies on the estimated nitrous oxide emission from wastewater treatment plants, Water Res. 47 (2013) 3120-3130. doi:10.1016/j.watres.2013.03.016.

[7] P. Wunderlin, J. Mohn, A. Joss, L. Emmenegger, H. Siegrist, Mechanisms of N_2O production in biological wastewater treatment under nitrifying and denitrifying conditions, Water Res. 46 (2012) 1027-1037. doi:10.1016/j.watres.2011.11.080.

[8] P. Wunderlin, M.F. Lehmann, H. Siegrist, B. Tuzson, A. Joss, L. Emmenegger, J. Mohn, Isotope Signatures of N_2O in a Mixed Microbial Population System: Constraints on N_2O Producing Pathways in Wastewater Treatment, Environ. Sci. Technol. 47 (2013) 1339-1348. doi:10.1021/es303174x.

[9] B.J. Ni, Z. Yuan, Recent advances in mathematical modeling of nitrous oxides emissions from wastewater treatment processes, Water Res. 87 (2015) 336-346. doi:10.1016/j.watres.2015.09.049.

[10] M.J. Kampschreur, H. Temmink, R. Kleerebezem, M.S.M. Jetten, M.C.M. van Loosdrecht, Nitrous oxide emission during wastewater treatment, Water Res. 43 (2009) 4093-4103. doi:10.1016/j.watres.2009.03.001.

[11] J. Desloover, S.E. Vlaeminck, P. Clauwaert, W. Verstraete, N. Boon, Strategies to mitigate N_2O emissions from biological nitrogen removal systems, Curr. Opin. Biotechnol. 23 (2012) 474-482. doi:10.1016/j.copbio.2011.12.030.

[12] T.M. Massara, S. Malamis, A. Guisasola, J.A. Baeza, C. Noutsopoulos, E. Katsou, A review on nitrous oxide (N_2O) emissions during biological nutrient removal from municipal wastewater and sludge reject water, Sci. Total Environ. 596-597 (2017) 106-123. doi:10.1016/j.scitotenv.2017.03.191.

[13] Y. Law, L. Ye, Y. Pan, Z. Yuan, Nitrous oxide emissions from wastewater treatment processes., Philos. Trans. R. Soc. Lond. B. Biol. Sci. 367 (2012) 1265-77. doi:10.1098/rstb.2011.0317.

[14] R. Marques, A. Rodríguez-Caballero, A. Oehmen, M. Pijuan, Assessment of online monitoring strategies for measuring N_2O emissions from full-scale wastewater treatment systems, Water Res. 99 (2016) 171-179. doi:10.1016/j.watres.2016.04.052.

[15] Y. Lim, D.-J. Kim, Quantification method of N_2O emission from full-scale biological nutrient removal wastewater treatment plant by laboratory batch reactor analysis., Bioresour. Technol. 165 (2014) 111-115. doi:10.1016/j.biortech.2014.03.021.

[16] A. Rodríguez-Caballero, I. Aymerich, M. Poch, M. Pijuan, Evaluation of process conditions triggering emissions of green-house gases from a biological wastewater treatment system, Sci. Total Environ. 493 (2014) 384-391. doi:10.1016/j.scitotenv.2014.06.015.

[17] M. Pocquet, Z. Wu, I. Queinnec, M. Spérandio, A two pathway model for N_2O emissions by ammonium oxidizing bacteria supported by the NO/N_2O variation, Water Res. 88 (2016) 948-959. doi:10.1016/j.watres.2015.11.029.

[18] B.-J. Ni, M. Ruscalleda, C. Pellicer-Nàcher, B.F. Smets, Modeling Nitrous Oxide Production during Biological Nitrogen Removal via Nitrification and Denitrification: Extensions to the General ASM Models, Environ. Sci. Technol. 45 (2011) 7768-7776. doi:10.1021/es201489n.

[19] K.E. Mampaey, B. Beuckels, M.J. Kampschreur, R. Kleerebezem, M.C.M. van Loosdrecht, E.I.P. Volcke, Modelling nitrous and nitric oxide emissions by autotrophic ammonia-oxidizing bacteria, Environ. Technol. 34 (2013) 1555-1566. doi:10.1080/09593330.2012.758666.

[20] Y. Law, B.J. Ni, P. Lant, Z. Yuan, N_2O production rate of an enriched ammonia-oxidising bacteria culture exponentially correlates to its ammonia oxidation rate, Water Res. 46 (2012) 3409-3419. doi:10.1016/j.watres.2012.03.043.

[21] B.-J. Ni, L. Ye, Y. Law, C. Byers, Z. Yuan, Mathematical modeling of nitrous oxide (N_2O) emissions from full-scale wastewater treatment plants., Environ. Sci. Technol. 47 (2013) 7795-7803. doi:10.1021/es4005398.

[22] K. Chandran, L.Y. Stein, M.G. Klotz, M.C.M. van Loosdrecht, Nitrous oxide production by lithotrophic ammonia-oxidizing bacteria and implications for engineered nitrogen-removal systems, Biochem. Soc. Trans. 39 (2011) 1832 LP-1837. http://www.biochemsoctrans.org/content/39/6/1832.abstract.

[23] B.-J. Ni, L. Peng, Y. Law, J. Guo, Z. Yuan, Modeling of Nitrous Oxide Production by Autotrophic Ammonia-Oxidizing Bacteria with Multiple Production Pathways, Environ. Sci. Technol. 48 (2014) 3916-3924. doi:10.1021/es405592h.

[24] W.C. Hiatt, C.P.L. Grady, An updated process model for carbon oxidation, nitrification, and denitrification., Water Environ. Res. 80 (2008) 2145-2156. doi:10.2175/106143008X304776.

[25] Y. Pan, B.J. Ni, Z. Yuan, Modeling electron competition among nitrogen oxides reduction and N_2O accumulation in denitrification, Environ. Sci. Technol. 47 (2013) 11083-11091. doi:10.1021/es402348n.

[26] B.J. Ni, Y. Pan, B. Van Den Akker, L. Ye, Z. Yuan, Full-Scale Modeling Explaining Large Spatial Variations of Nitrous Oxide Fluxes in a Step-Feed Plug-Flow Wastewater Treatment Reactor, Environ. Sci. Technol. 49 (2015) 9176-9184. doi:10.1021/acs.est.5b02038.

[27] J. Guerrero, A. Guisasola, J.A. Baeza, The nature of the carbon source rules the competition between PAO and denitrifiers in systems for simultaneous biological nitrogen and phosphorus removal, Water Res. 45 (2011) 4793-4802. doi:10.1016/j.watres.2011.06.019.

[28] V.C. Machado, J. Lafuente, J.A. Baeza, Activated sludge model 2d calibration with full-scale WWTP data: Comparing model parameter identifiability with influent and operational uncertainty, Bioprocess Biosyst. Eng. 37 (2014) 1271-1287. doi:10.1007/s00449-013-1099-8.

[29] M. Henze, W. Gujer, T. Mino, M.C.M. van Loosdrecht, Activated Sludge Models ASM1, ASM2, ASM2d, and ASM3, IWA Scientific and Technical Report n.9., IWA Publishing, London, 2000.

[30] I. Takács, G.G. Patry, D. Nolasco, A dynamic model of the clarification-thickening process, Water Res. 25 (1991) 1263-1271. doi:10.1016/0043-1354(91)90066-Y.

[31] I. Jubany, J. Carrera, J. Lafuente, J.A. Baeza, Start-up of a nitrification system with automatic control to treat highly concentrated ammonium wastewater: Experimental results and modeling, Chem. Eng. J. 144 (2008) 407-419. doi:10.1016/j.cej.2008.02.010.

[32] S. Capela, M. Roustan, A. Heduit, Transfer number in fine bubble diffused aeration systems, Water Sci. Technol. 43 (2001) 145-152.

[33] D.R. Lide, CRC Handbook of Chemistry and Physics, 87th ed., CRC Press/Taylor and Francis Group, Boca Raton, 2007.

[34] H. Hauduc, L. Rieger, I. Takács, A. Héduit, P.A. Vanrolleghem, S. Gillot, A systematic approach for model verification: application on seven published activated sludge models, Water Sci. Technol. 61(2010) 825-839. doi: 10.2166/wst.2010.898

[35] P. Reichert, P.A. Vanrolleghem, Identifiability and uncertainty analysis of the river water quality model no. 1 (RWQM1), Water Sci. Technol. 43 (2001) 329-338.

[36] U. Wiesmann, Biological nitrogen removal from wastewater, in: A. Fiechter (Eds.), Advances in Biochemical Engineering Bio- technology, Springer-Verlag, Berlin, 1994, pp. 113-154.

[37] A. Guisasola, M. Marcelino, R. Lemaire, J.A. Baeza, Z. Yuan, Modelling and simulation revealing mechanisms likely responsible for achieving the nitrite pathway through aeration control, Water Sci. Technol. 61 (2010) 1459-1465. doi: 10.2166/wst.2010.017

[38] G. Tallec, J. Garnier, G. Billen, M. Gousailles, Nitrous oxide emissions from secondary activated sludge in nitrifying conditions of urban wastewater treatment plants: Effect of oxygenation level, Water Res. 40 (2006) 2972-2980. doi:10.1016/j.watres.2006.05.037.

[39] M.J. Kampschreur, W.R.L. van der Star, H.A. Wielders, J.W. Mulder, M.S.M. Jetten, M.C.M. van Loosdrecht, Dynamics of nitric oxide and nitrous oxide emission during full-scale reject water treatment, Water Res. 42 (2008) 812-826. doi:10.1016/j.watres.2007.08.022.

[40] Y. Law, P. Lant, Z. Yuan, The confounding effect of nitrite on N_2O production by an enriched ammonia-oxidizing culture, Environ. Sci. Technol. 47 (2013) 7186-7194. doi:10.1021/es4009689.

[41] L. Peng, B.J. Ni, D. Erler, L. Ye, Z. Yuan, The effect of dissolved oxygen on N_2O production by ammonia-oxidizing bacteria in an enriched nitrifying sludge, Water Res. 66 (2014) 12-21. doi:10.1016/j.watres.2014.08.009.

[42] A. Aboobakar, E. Cartmell, T. Stephenson, M. Jones, P. Vale, G. Dotro, Nitrous oxide emissions and dissolved oxygen profiling in a full-scale nitrifying activated sludge treatment plant, Water Res. 47 (2013) 524-534. doi:10.1016/j.watres.2012.10.004.

[43] G. Dotro, B. Jefferson, M. Jones, P. Vale, E. Cartmell, T. Stephenson, A review of the impact and potential of intermittent aeration on continuous flow nitrifying activated sludge, Environ. Technol. 32 (2011) 1685-1697. doi:10.1080/09593330.2011.597783.

[44] I. Jubany, J. Lafuente, J.A. Baeza, J. Carrera, Total and stable washout of nitrite oxidizing bacteria from a nitrifying continuous activated sludge system using automatic control based on Oxygen Uptake Rate measurements, Water Res. 43 (2009) 2761-2772. doi:10.1016/j.watres.2009.03.022.

[45] O. Turk, D.S. Mavinic, Benefits of using selective inhibition to remove nitrogen from highly nitrogenous wastes, Environ. Technol. Lett. 8 (1987) 419-426. doi:10.1080/09593338709384500.

[46] Y. Peng, G. Zhu, Biological nitrogen removal with nitrification and denitrification via nitrite pathway, Appl. Microbiol. Biotechnol. 73 (2006) 15-26. doi:10.1007/s00253-006-0534-z.

[47] G. Ruiz, D. Jeison, R. Chamy, Nitrification with high nitrite accumulation for the treatment of wastewater with high ammonia concentration, Water Res. 37 (2003) 1371-1377.

[48] A. Guisasola, I. Jubany, J.A. Baeza, J. Carrera, J. Lafuente, Respirometric estimation of the oxygen affinity constants for biological ammonium and nitrite oxidation, J. Chem. Technol. Biotechnol. 80 (2005) 388-396. doi:10.1002/jctb.1202.

[49] M. Soliman, A. Eldyasti, Development of partial nitrification as a first step of nitrite shunt process in a Sequential Batch Reactor (SBR) using Ammonium Oxidizing Bacteria (AOB)

controlled by mixing regime, Bioresour. Technol. 221 (2016) 85-95. doi:10.1016/j.biortech.2016.09.023.

[50] M. Pijuan, J. Torà, A. Rodríguez-Caballero, E. César, J. Carrera, J. Pérez, Effect of process parameters and operational mode on nitrous oxide emissions from a nitritation reactor treating reject wastewater, Water Res. 49 (2014) 23-33. doi:10.1016/j.watres.2013.11.009.

[51] R.M.L.D. Rathnayake, M. Oshiki, S. Ishii, T. Segawa, H. Satoh, S. Okabe, Effects of dissolved oxygen and pH on nitrous oxide production rates in autotrophic partial nitrification granules, Bioresour. Technol. 197 (2015) 15-22. doi:10.1016/j.biortech.2015.08.054.

[52] N. Frison, A. Chiumenti, E. Katsou, S. Malamis, D. Bolzonella, F. Fatone, Mitigating off-gas emissions in the biological nitrogen removal via nitrite process treating anaerobic effluents, J. Clean. Prod. 93 (2015) 126-133. doi:http://dx.doi.org/10.1016/j.jclepro.2015.01.017.

[53] G. Mannina, A. Cosenza, D. Di Trapani, V.A. Laudicina, C. Morici, H. Ødegaard, Nitrous oxide emissions in a membrane bioreactor treating saline wastewater contaminated by hydrocarbons, Bioresour. Technol. 219 (2016) 289-297. doi:10.1016/j.biortech.2016.07.124.

[54] J.G. Kuenen, Anammox bacteria: from discovery to application., Nat. Rev. Microbiol. 6 (2008) 320-326. doi:10.1038/nrmicro1857.

[55] L. Peng, B.-J. Ni, L. Ye, Z. Yuan, The combined effect of dissolved oxygen and nitrite on N_2O production by ammonia oxidizing bacteria in an enriched nitrifying sludge, Water Res. 73 (2015) 29-36. doi:10.1016/j.watres.2015.01.021.

[56] Y. Jin, D. Wang, W. Zhang, Effects of substrates on N_2O emissions in an anaerobic ammonium oxidation (anammox) reactor, Springerplus. (2016) 1-12. doi:10.1186/s40064-016-2392-1.

[57] J.M. Garrido, W.A.J. Van Benthum, M.C.M. Van Loosdrecht, J.J. Heijnen, Influence of dissolved oxygen concentration on nitrite accumulation in a biofilm airlift suspension reactor, Biotechnol. Bioeng. 53 (1997) 168-178. doi:10.1002/(SICI)1097-0290(19970120)53:2<168::AID-BIT6>3.0.CO;2-M.

[58] W. Bae, S. Baek, J. Chung, Y. Lee, Optimal operational factors for nitrite accumulation in batch reactors, Biodegradation. 12 (2001) 359-366. doi:10.1023/A:1014308229656.

[59] G. Ciudad, O. Rubilar, P. Muñoz, G. Ruiz, R. Chamy, C. Vergara, D. Jeison, Partial nitrification of high ammonia concentration wastewater as a part of a shortcut biological nitrogen removal process, Process Biochem. 40 (2005) 1715-1719. doi:10.1016/j.procbio.2004.06.058.

[60] R. Blackburne, Z. Yuan, J. Keller, Partial nitrification to nitrite using low dissolved oxygen concentration as the main selection factor, Biodegradation. 19 (2008) 303-312. doi:10.1007/s10532-007-9136-4.

[61] M. Pan, Z. Hu, R. Liu, X. Zhan, Effects of loading rate and aeration on nitrogen removal and N_2O emissions in intermittently aerated sequencing batch reactors treating slaughterhouse wastewater at 11 ºC, Bioprocess Biosyst. Eng. 38 (2015) 681-689. doi:10.1007/s00449-014-1307-1.

[62] D.J.W. De Pauw, Optimal Experimental Design for Calibration of Bioprocess Models: A Validated Software Toolbox, PhD thesis in Applied Biological Sciences, University of Gent, Belgium. http://biomath.urgent.be/publications/download/, 2005 (accessed 17.06.17).

Development of an ASM2d-N_2O model to describe nitrous oxide emissions in municipal WWTPs under dynamic conditions

Theoni Maria Massara [a,b], Borja Solís [c], Albert Guisasola [c], Evina Katsou [a,b], Juan Antonio Baeza [c]

[a] Department of Mechanical, Aerospace and Civil Engineering, Brunel University London, Uxbridge Campus, Middlesex, UB8 3PH, Uxbridge, UK.

[b] Institute of Environment, Health and Societies, Brunel University London, Kingston Lane, Middlesex, UB8 3PH, Uxbridge, UK.

[c] GENOCOV. Departament d'Enginyeria Química, Biològica i Ambiental, Escola d'Enginyeria, Universitat Autònoma de Barcelona, Cerdanyola del Vallés (Barcelona), 08193, Barcelona, Spain.

Corresponding Author:

Prof. Juan Antonio Baeza,

Email: JuanAntonio.Baeza@uab.cat, Tel.: +34 93 581 1587

Abstract

Nitrous oxide (N_2O), a significant contributor to the greenhouse effect, is generated during the biological nutrient removal in wastewater treatment plants (WWTPs). Developing mathematical models estimating the N_2O dynamics under changing operational conditions (e.g. dissolved oxygen, DO) is essential to design mitigation strategies. Based on the activated sludge models (ASM) structure, this work presents an ASM2d-N_2O model including all the biological N_2O production pathways for a municipal WWTP under an anaerobic/anoxic/oxic (A^2/O) configuration with biological removal of organic matter, nitrogen and phosphorus, and its application in different dynamic scenarios. Three microbial N_2O production pathways were considered: nitrifier denitrification, hydroxylamine oxidation, and heterotrophic denitrification, with the first two being activated by ammonia oxidizing bacteria (AOB). A stripping effectivity (SE) coefficient was added to reflect the non-ideality of the stripping modeling. With the DO in the aerobic compartment ranging from 1.8 to 2.5 mg L^{-1}, partial nitrification and high N_2O production via nitrifier denitrification were noted, indicating that low aeration strategies lead to a low overall carbon footprint only if complete nitrification is not hindered. High N_2O emissions were predicted as a combination of low DO (~1.1 mg L^{-1}) with high ammonium concentration. With the AOB prevailing over the Nitrite Oxidizing Bacteria (NOB), nitrite was accumulated, thus activating the nitrifier denitrification pathway. After suddenly increasing the influent ammonium load, the AOB had a greater growth compared to the NOB and the same pathway was considered as N_2O hotspot. Especially under conditions promoting partial nitrification (i.e. low DO) and raising the stripping effect importance (i.e. high SEs), the highest N_2O emission factors were predicted.

Keywords A^2/O, nitrous oxide, emission factor, modeling, N_2O production pathways, N_2O stripping

Abbreviations

A^2/O	Anaerobic/Anoxic/Oxic WWTP configuration
AOB	Ammonia Oxidizing Bacteria
AOR	Ammonium Oxidation Rate
ASM	Activated Sludge Models
ASMN	Activated Sludge Model for Nitrogen
BNR	Biological Nutrient Removal
C	Carbon
COD	Chemical Oxygen Demand
DO	Dissolved Oxygen
EF	Emission Factor
EBPR	Enhanced Biological Phosphorus Removal
GHG	Greenhouse Gas
GWP	Global Warming Potential
HRT	Hydraulic Retention Time
IWA	International Water Association
N	Nitrogen
NOB	Nitrite Oxidizing Bacteria
OHO	Ordinary Heterotrophic Organisms
P	Phosphorus
PAO	Phosphorus Accumulating Organisms
PHA	Polyhydroxyalkanoates
PP	Polyphosphates
SA	Sensitivity Analysis
SBR	Sequencing Batch Reactor
SE	Stripping Effectivity
TKN	Total Kjeldahl Nitrogen
TSS	Total Suspended Solids
WWTP	Wastewater Treatment Plant

1. Introduction

Nitrous oxide (N_2O) is a particularly important greenhouse gas (GHG) because of its high global warming potential (GWP) compared to other GHGs such as methane (CH_4) and carbon dioxide (CO_2). N_2O has a GWP 265 times higher than CO_2, in contrast to CH_4 that has a GWP only 28 times higher than CO_2 [1]. Moreover, N_2O has been characterized as the predominant ozone-depleting substance of the century [2]. N_2O can be produced and directly emitted during the biological nutrient removal (BNR) in wastewater treatment plants (WWTPs) [3-4]. More importantly, it has been proved that the total carbon (C) footprint of full-scale WWTPs can be affected by N_2O emissions to an impressive extent: e.g. around 60% [5], or even around 75% [6].

The currently known microbial pathways for N_2O production during the BNR are connected to the biochemical processes of nitrification and denitrification. Those related to nitrification occur through the activity of the ammonia oxidizing bacteria (AOB) (i.e. the nitrifier denitrification and the hydroxylamine (NH_2OH) oxidation). Heterotrophic denitrification, during which N_2O is an intermediate product, is the third biological pathway [5, 7-9]. The parameters mostly contributing to the N_2O generation have been reviewed and linked to insufficient levels of dissolved oxygen (DO) at the nitrification stage, increased nitrite (NO_2^-) concentration during both nitrification and denitrification, in addition to low chemical oxygen demand to nitrogen ratio (COD/N) during denitrification [10-12].

Studies have revealed a considerable variation in the N_2O emission in WWTPs, thus rendering the emission factor (EF) estimation difficult. For example, Law et al. [13] reported an EF range of 0-25% amongst different full-scale WWTPs. The significant variation can be explained through the highly dynamic conditions in WWTPs, as well as the different configurations and operational conditions applied in each plant [13-14]. Furthermore, the N_2O EF calculation can be

influenced by the N_2O quantification method [13, 15]. After examining twelve different WWTPs in the United States, Ahn et al. [3] found that the EFs ranged from 0.01 to 1.8% when normalized to the influent Total Kjeldahl Nitrogen (TKN) load. This variability was correlated with the diurnal variations of the influent N-loading. Similarly, Rodriguez-Caballero et al. [16] examined the N_2O dynamics in a municipal WWTP. Due to instable nitrification in the bioreactor, the emissions presented a significant decreasing trend within the day; the reported N_2O EF decreased from 0.116 to 0.064% of the influent TKN. In both cases, the authors captured the changing N_2O dynamics because of the continuous online reporting of the data. Foley et al. [4] studied seven full-scale BNR WWTPs in Australia with various configurations, concluding to a minimum N_2O EF of 0.6% and a maximum of 25.3% of the N-denitrified. The authors recommended online emission monitoring in the biological compartments for the in-depth understanding of the influent dynamics and process characteristics in WWTPs. Daelman et al. [6] examined different monitoring scenarios on a 16-month dataset of a fully covered WWTP in the Netherlands to conclude to the most accurate and cost-effective one. The estimation of the average annual N_2O emission required the description of seasonal dynamics and, thus, the acquisition of long-term, online or grab samples (the latter including nightly and weekend sampling). On the other hand, short-term campaigns focusing on the diurnal trends proved to be more expensive since they called for high-frequency online sampling. Thus, the accurate estimation of the N_2O EF within a WWTP is a highly challenging task depending on various factors such as the operational conditions, the configuration type, the quantification method, the sampling strategy, etc.

The development of mathematical tools for the prediction of N_2O emissions during the operation of WWTPs seems essential to allow the study of different scenarios. The simulation of N_2O production allows the optimization of BNR processes, thus facilitating the decrease of N_2O

emissions. N_2O modeling is constantly advancing; models describing different pathways and based on different assumptions have been developed [9, 17].

For instance, models that focus on the nitrifier denitrification pathway have been suggested: Ni et al. [18] developed a model describing how low DO levels (i.e. ≤1.5 mg L^{-1}) can inhibit complete nitrification, induce NO_2^- accumulation and, subsequently, increase N_2O emissions. Similarly, Mampaey et al. [19] observed that N_2O production and emission was mainly observed during the aerated phases under relatively low DO (i.e. ≤1.5 mg L^{-1}). The NH_2OH oxidation pathway was the basis for the models by Law et al. [20] and Ni et al. [21]. Law et al. [20] observed the N_2O production rate increasing with the ammonium oxidation rate (AOR) within an enriched AOB culture. The simulations by Ni et al. [21] indicated that ammonium (NH_4^+) accumulation during aeration was translated into a high specific AOR and, finally, into the increased production of by-products such as NH_2OH.

Given that the AOB pathways are regarded as major contributors to the N_2O production amongst the three microbial routes [7, 17, 22], 2-(AOB) pathway models have emerged. For example, the Ni et al. [23] model which depicted the following trends: (i) NH_2OH oxidation predominance under extremely low/high NO_2^- concentration along with high DO, and (ii) nitrifier denitrification predominance at low DO with moderate NO_2^- accumulation. In the 2-AOB pathway model by Pocquet et al. [17], the DO increase was combined with decreased N_2O emission along with a slightly higher contribution of the NH_2OH oxidation pathway.

Regarding the heterotrophic denitrification pathway, the activated sludge model for nitrogen (ASMN) developed by Hiatt and Grady [24] described denitrification as a four-step reaction with different specific growth rates. In a more recent model, Pan et al. [25] considered the electron

competition amongst the four heterotrophic denitrification steps by dissociating the C-oxidation and the N-reduction.

Nevertheless, N_2O is likely to be produced/consumed by both the AOB and the heterotrophic denitrifiers during the BNR in WWTPs. As a result, the development of models including all the possible pathways gives a deeper insight into the N_2O production/consumption dynamics and enhances the study of strategies for the N_2O emission mitigation, especially in cases of full-scale modeling [9-10, 12]. With the view to investigating the significant spatial variations in the N_2O flux of a step-feed 2-pass full-scale activated sludge plant, Ni et al. [26] combined the 2-(AOB) pathway modeling part by Ni et al. [23] and the heterotrophic denitrification processes appearing in Ni et al. [21] in an integrated model.

Multiple-pathway models seem more apt to elucidate the effect of changing operational parameters (e.g. DO, NO_2^- concentration, etc.) and explain possible spatial/temporal variations, thus helping plant operators with designing mitigation strategies [12]. Given the influence of aeration and DO profiles on the emissions, it is necessary to develop even more integrated models which include all the production pathways and, simultaneously, consider the N_2O transfer from the liquid to the gas phase under varying gas flow patterns.

The activated sludge models (ASM) introduced by the International Water Association (IWA) task group have been widely used for the description of BNR processes during wastewater treatment [12]. Extensions to these models have been made to consider the N_2O production with emphasis either on the nitrifier denitrification or the NH_2OH oxidation pathway, and on the impact of changing influent (e.g. influent N-loading, COD/N) and/or operational conditions (e.g. DO) [18, 21]. Nevertheless, these models lack consideration of other nutrients removal (e.g. P). Moreover, they do not necessarily pay equal attention to all biological N_2O production routes

and/or deal with the N_2O stripping modeling. Hence, the aim of this work was to develop an ASM-type model which: (i) includes N, P and organic matter removal, (ii) integrates all the microbial pathways for N_2O production/consumption, (iii) contains N_2O stripping modeling, and (iv) estimates the N_2O EF under different DO levels. To this end, the IWA ASM2d model was modified and expanded into an ASM2d-N_2O model to include all the biological N_2O production pathways and the calculation of the N_2O EF. The continuity of the model was also examined to detect typing and/or conceptual errors, inconsistencies and gaps in the proposed model. Finally, sensitivity analysis (SA) was performed to reveal the parameters most sensitive to the N_2O EF as estimated using the proposed model.

2. Materials and methods

2.1 Brief description of the WWTP configuration and influent data

The kinetic model was developed to describe the simultaneous N, P and COD removal for a WWTP with three continuous stirred tank reactors and one settler operating as an anaerobic-anoxic-aerobic (A^2/O) configuration (Fig. 1).

The first reactor (Hydraulic Retention Time: HRT=1.6 h) was anaerobic with the view to facilitating the phosphorus accumulating organisms (PAO) predominance over the ordinary heterotrophic organisms (OHO) and, subsequently, enhancing the P-removal. Nitrate (NO_3^-) entering the second (anoxic) reactor (HRT=1.6 h) through the internal recycle of the mixed liquor was denitrified by the OHO or the denitrifying PAO. Finally, the third (aerobic) reactor (HRT=5 h) coupled P and organic matter removal along with nitrification. After settling the treated effluent, the settler (HRT=2.9 h) produced two streams; the effluent and an external

recycle of biomass returned to the first reactor. The total WWTP HRT was 11.1 h, and the purge, internal and external recirculation ratios with respect to the influent flowrate were equal to 0.007, 2 and 1/3, respectively. The typical DO control setpoints for the three reactors were: 0 mg L^{-1} (anaerobic and anoxic) and 3 mg L^{-1} (aerobic).

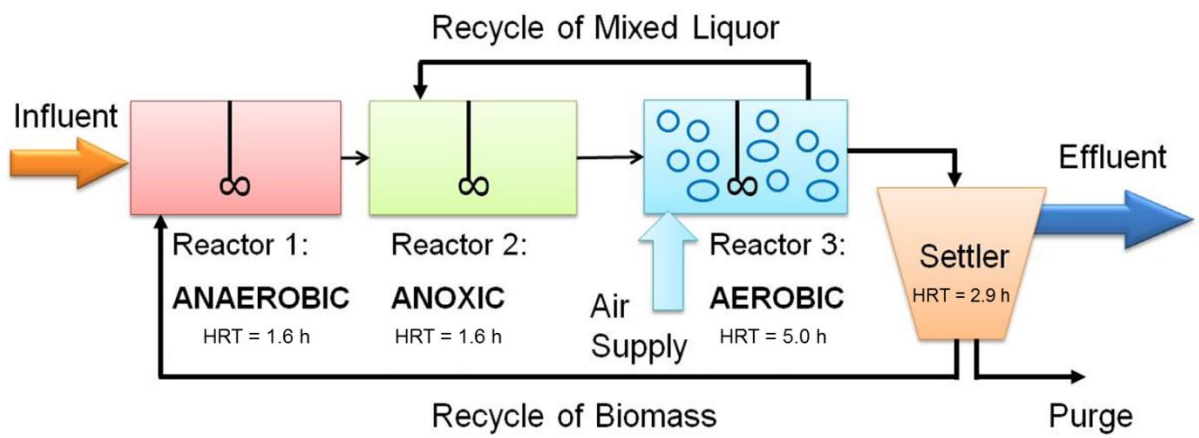

Figure 1. A^2/O WWTP configuration integrated in the current study (adapted from Guerrero et al. [27]).

The influent composition was typical for the municipal WWTP of Manresa (Catalonia, Spain) (Machado et al. [28]). The influent characterization considered S_I (inert soluble material), X_I (inert particulate organic material), X_S (slowly biodegradable substrates), and S_F (fermentable, readily biodegradable organic substrates) fractions as follows: S_I=0.07*COD, X_I=0.11*COD, X_S=0.6*COD, and S_F= 0.4*COD (Machado et al. [28]). All the remaining COD state variables were fixed to zero. The influent composition is shown in Table 1.

Table 1. Influent composition (pH=7 and T=20 ºC)

Composition	mg L^{-1}
$N\text{-}NH_4^+$	20
BOD_5	170
COD	420
Total N	35
$N\text{-}NO_3^-$	2.6
$P\text{-}PO_4^{3-}$	9
TKN (Kjeldahl N)	33
TSS	189

2.2 Model description

The core of our ASM2d-N_2O model emerged as an extension of the IWA ASM2d (i.e. an ASM version including the bioprocesses related to the heterotrophic biomass, the PAO and the nitrifiers) [29]. The scope of this study was to describe the N_2O production/consumption dynamics within a WWTP with enhanced biological phosphorus removal (EBPR). In that sense, the assumptions for the description of the two AOB pathways were made upon the Pocquet et al. [17] model, while those for the heterotrophic denitrification upon the Hiatt and Grady [24] model, always by extending and adapting the same processes to PAOs. It was considered as a holistic approach for the description of the N_2O dynamics during the BNR in WWTPs. Thus, the final model describes the following: N_2O production through all the three microbial pathways, but also N_2O consumption during denitrification (Fig. 2).

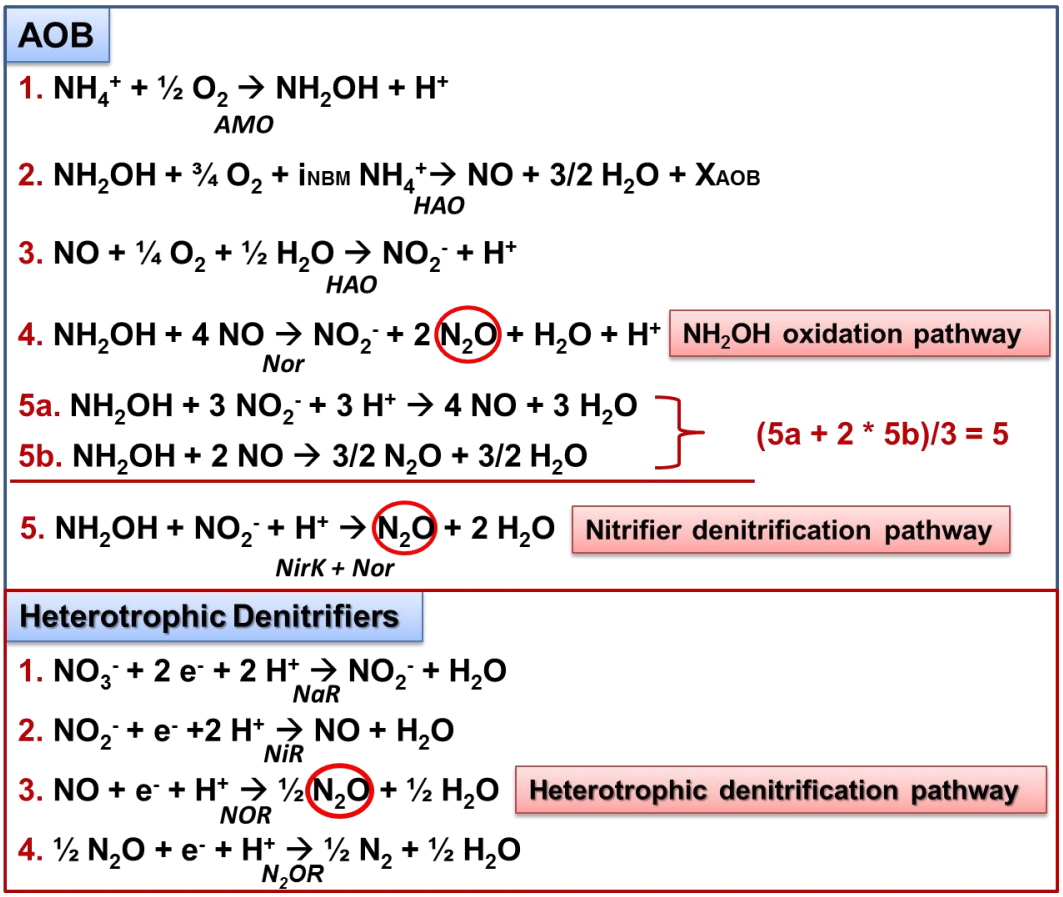

Figure 2. The three pathways for the N_2O production considered in our model: NH_2OH oxidation pathway (AOB pathway), nitrifier denitrification (AOB pathway) and heterotrophic denitrification. The assumptions concerning the AOB and heterotrophic denitrification-related reactions were made in accordance to what was reported by Pocquet et al. [17] and Ni and Yuan [9].

Considering the assumptions made by Pocquet et al. [17], our work included the following five AOB reactions (Fig. 2): (1) NH_4^+ oxidation to NH_2OH, (2) NH_2OH oxidation to nitric oxide (NO), (3) NO oxidation to NO_2^-, (4) NO reduction to N_2O along with the NH_2OH oxidation to NO_2^- (N_2O production via the NH_2OH oxidation pathway), (5) NO_2^- reduction combined with NH_2OH oxidation to produce N_2O (N_2O production by the nitrifier denitrification pathway,

combination of reactions 5a and 5b). The additional four reactions related to the heterotrophic denitrification pathway and the enzymes catalyzing all the steps of the three pathways are schematically shown in Fig. 2. The enzymes involved are: AMO (NH_4^+ monooxygenase), HAO (NH_2OH oxidoreductase), Nor (NO reductase), NirK (NO_2^- reductase) for the AOB, and NaR (NO_3^- reductase), NiR (NO_2^- reductase), NOR (NO reductase), and N_2OR (N_2O reductase) for the heterotrophs [9, 17]. Pocquet et al. [17] grouped together the NO_2^- reduction to NO (NirK enzyme) and the reduction of NO to N_2O (Nor enzyme) into one reaction: NO_2^- being directly reduced to N_2O (Fig. 2, eq. 5). They assumed that the Nor quickly consumed the NO produced by the aid of NirK or, equivalently, that the NO produced through the nitrifier denitrification pathway was converted to N_2O at a high rate. The latter was necessary in order to avoid a NO loop.

The model also considered P removal. Based on the ASM2d [29] structure, the following PAO-related processes were included: storage of polyhydroxyalkanoate (PHA), aerobic storage of polyphosphate (PP), aerobic growth of PAO and lysis of PHA, PP and PAO. Moreover, the anoxic processes of PP storage and PAO growth were expanded to cover all the four possible electron acceptors included in the current model: NO_3^-, NO_2^-, NO and N_2O, following the same reactions as those for the ordinary heterotrophs (Fig. 2).

The final model was developed in Matlab® using the *ode15s* function, which is a variable order method recommended for stiff systems. The settling was modeled with reference to the study by Takács et al. [30]. Steady-state was achieved by simulating the WWTP with constant influent composition for a period of 200 d.

All the kinetic parameter values were normalized for 20 ºC from the ASM2d section of Henze et al. [29]. The AOB decay and growth rates were taken from Hiatt and Grady [24]; μ_{AOB}=0.78 d^{-1}, b_{AOB}=0.096 d^{-1}. As far as the growth/decay rates for the nitrite oxidizing bacteria (NOB) are concerned, two different sets were tested for comparative purposes; the first from Hiatt and Grady [24] (μ_{NOB}=0.78 d^{-1}, b_{NOB}=0.096 d^{-1}), and the second one from Jubany et al. [31] (μ_{NOB}=1.02 d^{-1}, b_{NOB}=0.17 d^{-1}).

Tables presenting the stoichiometric/kinetic parameters, the stoichiometry, and the process rates of the processes integrated into our model are given in detail as Supportive Material.

2.3 N_2O emission factor (EF) modeling

The N_2O emission factor in our model was calculated in three ways: i) considering both the stripped N_2O and the N_2O in the effluent to reflect the most conservative estimation (N_2O-EF_{TOTAL}, Eq. 1.1), ii) considering only the stripping contribution (N_2O-EF_{GAS}, Eq. 1.2), and iii) considering only the effluent contribution (N_2O-EF_{EF}, Eq. 1.3).

$$\boldsymbol{N_2O\text{-}EF_{TOTAL}}(\%) = \mathbf{100} \cdot \frac{\boldsymbol{N_2O_{ST}+N_2O_{EF}}}{\boldsymbol{N_{IN}}} \quad \textbf{(Equation 1.1)}$$

$$\boldsymbol{N_2O\text{-}EF_{GAS}}\ (\%) = \mathbf{100} \cdot \frac{\boldsymbol{N_2O_{ST}}}{\boldsymbol{N_{IN}}} \quad \textbf{(Equation 1.2)}$$

$$\boldsymbol{N_2O\text{-}EF_{EF}}\ (\%) = \mathbf{100} \cdot \frac{\boldsymbol{N_2O_{EF}}}{\boldsymbol{N_{IN}}} \quad \textbf{(Equation 1.3)}$$

Where N_2O_{ST} is the amount of N_2O stripped from the aerobic reactor, N_2O_{EF} the N_2O in the effluent of the plant and N_{IN} the total N-content of the influent, which was calculated with Eq. 2.

$$N_{IN}\ (gN \cdot d^{-1}) = Q_{IN} \cdot (S_{NH4} + S_{NO3} + S_F \cdot i_{NS_F} + X_S \cdot i_{NX_S} + S_I \cdot i_{NS_I} + X_I \cdot i_{NX_I})$$

(Equation 2)

With Q_{IN} as the influent flowrate, and the rest of terms following the ASM2d nomenclature reported by Henze et al. [29]: S_{NH4}, S_{NO3}, S_F, X_S, S_I and X_I denote the influent concentrations for NH_4^+ (gNH_4^+-N m^{-3}), NO_3^- (gNO_3^--N m^{-3}), fermentable substrate (gCOD m^{-3}), slowly biodegradable substrate (gCOD m^{-3}), inert soluble substrate (gCOD m^{-3}) and inert particulate substrate (gCOD m^{-3}), respectively. i_{NS_F}, i_{NX_S}, i_{NS_I} and i_{NX_I} are the N-content (gN g^{-1}COD) of S_F, X_S, S_I and X_I, respectively.

The N_2O in the effluent (N_2O_{EF}) was calculated using the N_2O concentration (gN m^{-3}) in the aerobic reactor (N_2O_{AE}) as in Eq. 3:

$$N_2O_{EF}\ (gN \cdot d^{-1}) = Q_{IN} \cdot N_2O_{AE} \qquad \textbf{(Equation 3)}$$

Finally, the stripped N_2O (N_2O_{ST}) was calculated using Eq. 4, where k_La_{N2O} is the volumetric mass transfer coefficient for N_2O, V_{AE} is the volume of the aerobic reactor and the SE factor denotes 'stripping effectivity'. We applied SE values in the range 0-1 as a mechanism enabling us to investigate the impact of the non-ideality of this typical simplified modeling approach on the N_2O EF.

$$N_2O_{ST}\ (gN \cdot d^{-1}) = k_La_{N_2O} \cdot V_{AE} \cdot N_2O_{AE} \cdot SE \qquad \textbf{(Equation 4)}$$

The volumetric mass transfer coefficient (k_La) comprises the global transfer coefficient k_L along with the interfacial area a (interphase transport surface between liquid and gas per unit of reactor volume). The k_La_{N2O} resulted from Eq. 5 following Higbie's penetration model [32]:

$$\boldsymbol{k_L a_{N_2O}(d^{-1}) = k_L a_{O_2} \cdot \sqrt{\frac{Dif_{N2O}}{Dif_{O2}}}} \qquad \textbf{(Equation 5)}$$

$k_La_{O_2}$ is the volumetric mass transfer of oxygen in the aerobic reactor, which was automatically calculated by including the DO control system in the model. Dif_{N2O} is the molecular diffusivity of N_2O in water ($2.11 \cdot 10^{-9}$ m^2 s^{-1} at 20 ºC) and Dif_{O2} the molecular diffusivity of oxygen in water ($2.01 \cdot 10^{-9}$ m^2 s^{-1} at 20 ºC) [33].

2.4 Continuity check

The continuity of the model was verified to detect typos, inconsistencies, gaps or conceptual errors in the proposed extension following the methodology proposed by Hauduc et al. [34] who checked and corrected seven of the most commonly used ASM models. The method consists in the analysis of the matrix which results after multiplying the stoichiometric matrix (available in the Supportive Material section) and the composition matrix (i.e. conversion factors of each state variable to COD, N, P, charge and total suspended solids (TSS)). The tolerance allowing the acceptance of the continuity matrix was set at 10^{-15} as suggested by Hauduc et al. [34]. The stoichiometric matrix, the composition matrix (definitions and numerical values) and the continuity check can be found in the Supportive Material.

2.5 Sensitivity analysis (SA)

A local SA was conducted to establish the parameters that were more sensitive to $N_2O\text{-}EF_{TOTAL}$ (Eq. 1.1). Reichert and Vanrolleghem [35] defined the relative sensitivity ($S_{i,j}$) of an output (y_i) with respect to a parameter (θ_j) as in Eq. 6:

$$\mathbf{S_{i,j} = \frac{\theta_j}{y_i} \cdot \frac{\partial y_i}{\partial \theta_j}} \qquad \textbf{(Equation 6)}$$

In our case, the $N_2O\text{-}EF_{TOTAL}$ at steady state was used as the model output. The parameters involved in the SA were all the kinetic and stoichiometric parameters as well as the conversion factors that are given in the Supportive Material. However, the S_I production in hydrolysis (f_{SI}) and the P-content of S_I (i_{PSI}) were excepted since they were fixed at zero. Furthermore, the anoxic growth factor (n_G) parameter was adjusted to 0.9 (instead of 1) to compute the forward difference. The NOB growth and decay parameters were retrieved from the study by Hiatt and Grady [24]. A total number of 104 parameters were included in the SA.

The central difference method was used to calculate the sensitivity for each parameter. Different perturbation factors, ranging from 0.01% to 10%, were tested to ensure that the perturbation factor selection did not affect the parameter ranking.

As will be discussed in sections 3.1, 3.2 and 3.4, different DO values in the aerobic reactor (e.g. varying from 1 to 4 mg L^{-1}), resulted in very different EFs. Hence, the SA was performed under two different steady-state scenarios (i.e. at high and low DO setpoint in the aerobic reactor, set as equal to 3 and 1 mg L^{-1}, respectively). The latter was decided to better understand the causes of

high N_2O emission. During the SA tests, the influent S_{NH4} was fixed at 30 mg L^{-1} and the SE at 0.5.

3. Results and discussion

3.1 DO impact on nitrification and N_2O emissions

The model was applied to investigate the effect of DO concentration (from 0 to 4 mg L^{-1}) in the aerobic reactor on the nitrification process and, finally, on the N_2O emissions. The evolution of N_2O-EF_{TOTAL}, AOB and NOB activity and NH_4^+, NO_2^- and NO_3^- concentrations with respect to different DO levels are shown in Fig. 3.

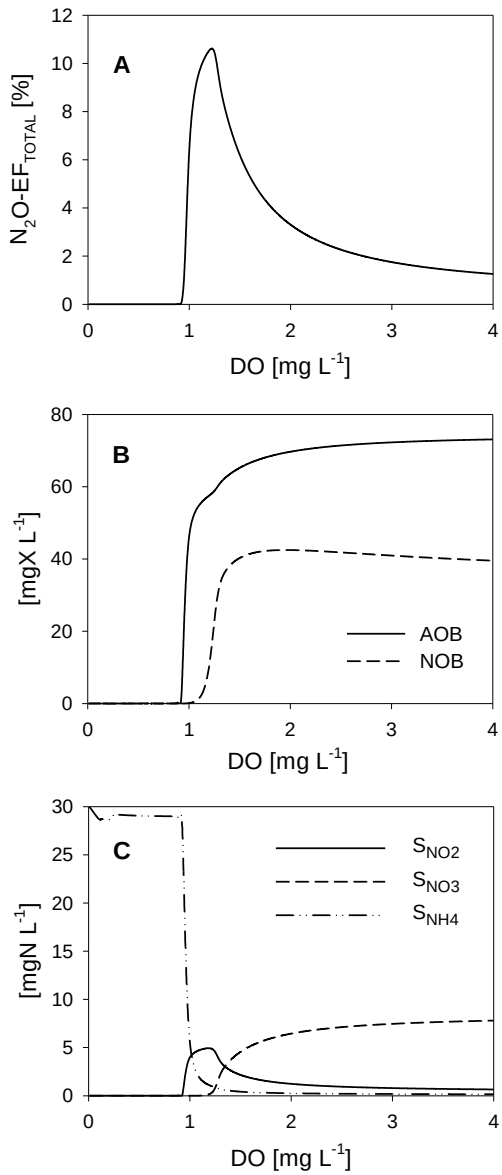

Figure 3. DO effect in the aerobic reactor on the steady state values of (A) N_2O emission factor, (B) AOB and NOB concentration, and (C) NO_2^-, NO_3^- and NH_4^+, concentration. The SE was 1 and both the AOB and NOB growth and decay parameters were taken from the study by Hiatt and Grady [24].

Fig. 3B and 3C show that neither AOB/NOB growth nor NO_2^-/NO_3^- production was observed under oxygen-limiting conditions (i.e. for DO values lower than approximately 0.8 mg L^{-1}). The NH_4^+ concentration increased compared to the respective influent one (S_{NH4}=20 mgN L^{-1}) because of hydrolysis processes releasing NH_4^+ and no nitrification happening due to the low DO. The DO increase from 0.8 mg L^{-1} onwards enhanced the AOB growth. On the contrary, the NOB growth only commenced at a DO around 1.1 mg L^{-1} (Fig. 3B). These threshold values (i.e. 0.8 and 1.1 mg L^{-1}) are mainly determined by the oxygen affinity constants values and, thus, from mass transfer and operational conditions. The NOB have a lower affinity to oxygen compared to the AOB [36], which explains why synergies that result in partial nitrification/nitritation (i.e. NH_4^+ oxidation to NO_2^-) are based on the selection of a proper DO setpoint [37]. In accordance to this, our simulation results demonstrated that the AOB prevailed over the NOB under relatively low DO levels (i.e. DO between 0.8 and 1.1 mg L^{-1}) (Fig. 3B). In this range, the NH_4^+ concentration decreased, while NO_2^- started increasing; nitritation resulted in NO_2^- accumulation (Fig. 3C). Within the same DO range (0.8-1.1 mg L^{-1}), we observed a significant N_2O emission factor increase up to almost 10.5% (Fig. 3A). In this case, the dominant N_2O production pathway was nitrifier denitrification; under such oxygen-limiting conditions, NO_2^- substitutes oxygen at the role of the final electron acceptor and, thus, the AOB perform nitrifier denitrification [11, 38-39]. Our observations agree with previous studies investigating the preferred N_2O production pathway at different DO levels. For example, Law et al. [40] worked with an enriched AOB culture in a lab-scale nitritation system fed with anaerobic digester liquor; amongst the two AOB pathways, nitrifier denitrification was suggested as predominant at the lowest DO values tested (i.e. 0.55 and 1.3 mg L^{-1}; the highest tested was 2.3 mg L^{-1}) and decreased NO_2^- concentrations. Similarly, the DO effect on N_2O production by an

enriched nitrifying sludge was investigated in a lab-scale sequencing batch reactor (SBR); the DO increase from 0.2 to 3 mg L^{-1} was correlated with a decreased contribution of the nitrifier denitrification pathway [41].

Our simulations showed that, as soon as DO reached the level of 1.5 mg L^{-1}, AOB and NOB were stabilized around 70 mg L^{-1} and 40 mg L^{-1}, respectively (Fig. 3B). Complete nitrification started and resulted in less NO_2^- accumulation as well as in the gradual nitrifier denitrification pathway deactivation. This is depicted in Fig. 3A through a continuous N_2O-EF_{TOTAL} decrease that initiated at a DO around 1.5 mg L^{-1} and was reinforced with the further DO increase. Furthermore, NO_3^- production began; the latter indicating that full nitrification was happening (Fig. 3C). At high DO levels (i.e. >3 mg L^{-1}), the N_2O emission factor was significantly lower; less than 2%. In terms of N_2O emission mitigation, high DO (i.e. >3 mg L^{-1}) proved to be beneficial. However, it is an energy-consuming option. For instance, a study on a plug-flow (three-pass) full-scale municipal WWTP in the UK indicated that N_2O emissions added 13% to the carbon footprint of the plant because of the electricity needed to run the nitrifying process [42]. Intermittent aeration regimes can be applied as a promising option to reduce aeration costs by 33-45%. However, this strategy is likely to disturb the bioreactor operation, hinder the nitrifying population activity, and, hence, create conditions favouring the N_2O generation. Consequently, an additional carbon footprint related to the N_2O emissions can arise [43]. Therefore, it is essential to consider the potential magnitude of N_2O process emissions before adopting low-energy strategies [42]. Increased N_2O production and emission is probable under low-DO conditions suggesting a high final overall carbon footprint for a WWTP. It is useful to investigate multiple DO values to find an interval inside which neither the nitrification process

nor the plant's carbon footprint is compromised; this can be between 1.8 and 2.5 mg L^{-1} for our study.

3.2 Influence of two different parameter sets for the NOB growth and decay on the N_2O emission factor (EF)

As explained in section 2.2, two different sets regarding the growth/decay rates for the NOB were tested for comparative purposes; one from Hiatt and Grady [24] (μ_{NOB}=0.78 d^{-1}, b_{NOB}=0.096 d^{-1}) and the second one from Jubany et al. [31] (μ_{NOB}=1.02 d^{-1}, b_{NOB}=0.17 d^{-1}).

Short-cut biological nitrogen removal, i.e. nitritation (NH_4^+ oxidation to NO_2^-) followed by denitritation (NO_2^- reduction to N_2) emerged as extremely interesting in the domain of wastewater treatment, especially in the cases of wastewaters with high NH_4^+ content [44]. Compared to full nitrification (i.e. NH_4^+ oxidation to NO_3^-), the short-cut process has proved to be more advantageous in terms of COD demand (40% reduction during denitrification) and denitrification rate (63% higher) [45]. Furthermore, it can induce a 25% decrease in the oxygen demand during nitrification because of the avoidance of nitratation (i.e. NO_2^- oxidation to NO_3^-) [46]. If nitritation is the target for the plant operators, it is essential to apply conditions which favour the AOB activity but suppress the NOB community. The relative influential parameters include temperature, pH and DO [44]. The current study focused on the DO effect; temperature and pH were considered stable for all simulations (T=20 ºC and pH=7). Low-DO environments are expected to enhance the NO_2^- accumulation [47-49].

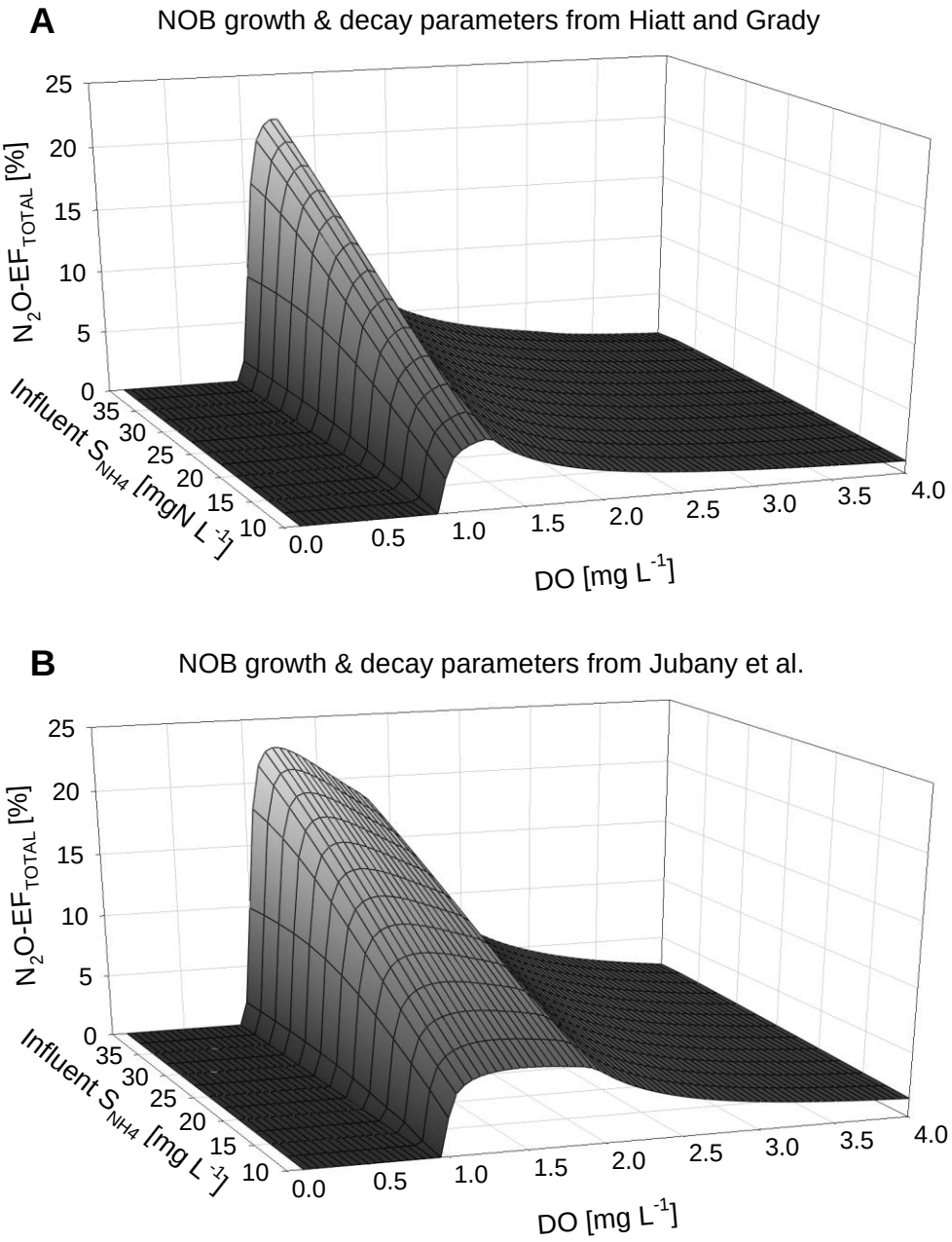

Figure 4. The steady-state N_2O emission factor with respect to different DO setpoints in the aerobic reactor (0 to 4 mg L^{-1}) and influent S_{NH4} concentrations (10 to 40 mg L^{-1}). The selected SE was 1. A) NOB parameters of Hiatt and Grady [24]. B) NOB parameters of Jubany et al. [31].

Fig. 4 shows the effect on N_2O-EF_{TOTAL} in different scenarios with the DO concentration ranging from 0 to 4 mg L^{-1} and the influent S_{NH4} from 10 to 40 mg L^{-1}. For this part of the simulations, we used the maximum theoretical stripping efficiency (SE=1). The latter offered the possibility to examine a range of DO and influent NH_4^+ values which embodied the worst-case scenario (i.e. highest N_2O emissions). The simulations were executed for each one of the different parameter sets for the NOB growth and decay. In both cases, the general trends were similar. First, no nitrification and, subsequently, no N_2O emission was noticed at very low DO (i.e. below 0.8 mg L^{-1}). The DO increase provided the conditions for the initiation of nitritation. The highest N_2O emissions occurred for (still relatively low) DO levels between 0.8 and 1.8 mg L^{-1}; it is when nitritation led to NO_2^- accumulation and, afterwards, to N_2O production through the nitrifier denitrification pathway. The model predicted the highest N_2O emission (around 22%) under the following combination: DO around 1.1 mg L^{-1}, influent N-NH_4^+=40 mg L^{-1} (i.e. the highest tested) and SE=1. The further DO increase above 1.8 mg L^{-1} resulted in the significant N_2O-EF_{TOTAL} decrease (reaching almost 2% after DO>2.5 mg L^{-1}), as a consequence of the NO_2^- consumption through full nitrification. Similar results have been reported in past experimental studies. Pijuan et al. [50] monitored the nitritation process in an airlift system with granular biomass to explore the DO effect. N_2O emissions decreased from 6% to 2.2% of N-oxidized when DO increased from 1 to 4.5 mg L^{-1}. Moreover, Rathnayake et al. [51] observed that the N_2O emissions over the oxidized NH_4^+ decreased from 2.9% (DO=0.6 mg L^1) to 1.4% (DO=2.3 mg L^1) in a lab-scale nitritation reactor fed with synthetic wastewater.

Furthermore, according to the trends noted while examining the N_2O-EF_{TOTAL} versus the influent S_{NH4} concentration, the N_2O emissions increased with the increase of the influent NH_4^+ load. As a result, lower loaded influents are expected to have lower emissions. While investigating the

combined effect of N-loading rate and DO in a pilot-scale SBR treating reject water, Frison et al. [52] tested two different combinations of these parameters (first combination: volumetric N-loading rate=1.08 kg N m^{-3} d^{-1} & DO=0.95 mg L^{-1}; second combination: volumetric N-loading rate=0.81 kg N m^{-3} d^{-1} & DO=1.48 mg L^{-1}). N_2O emissions decreased from 1.49% to 0.24% of the influent N-load when switching from the first to the second combination. The higher DO along with an influent N-loading not exceeding the system's capacity resulted in lower NO_2^- accumulation and N_2O emissions. Similarly, our model predicted the increase in N_2O emissions after applying higher S_{NH4} influent concentrations along with lower DO.

However, it is noted that the N-removal via NO_2^- was prolonged with the NOB growth and decay parameters from Jubany et al. [31]. Nitritation occurred at around 0.8<DO<1.8 mg L^{-1} with the parameters from Hiatt and Grady [24], whereas at around 0.8<DO<2.2 mg L^{-1} with the parameters from Jubany et al. [31] (Fig. 4). The NOB growth and decay rates of Jubany et al. [31] are 23.5% and 43.5% higher, respectively, than the ones of Hiatt and Grady [24]. However, the most important parameter affecting the N-removal via NO_2^- is the NOB-related half-saturation coefficient for oxygen. This parameter was 1.2 mg L^{-1} for Hiatt and Grady [24], whereas equal to 1.75 mg L^{-1} [44, 48] for Jubany et al. [31]. This higher value increases the range of DO values leading to a limitation of NOB activity, and hence provokes a higher operational region with important N_2O emission.

Finally, the results obtained in this section match with past experimental observations according to which the operational parameters mostly contributing to the N_2O generation are linked to insufficient DO levels at the nitrification stage and increased NO_2^- concentration during both nitrification and denitrification [10-12].

3.3 Effect of the stripping effectivity (SE) on the N_2O emission factor (EF)

Even though N_2O is an intermediate of heterotrophic denitrification, aerobic (nitrification-related) compartments in WWTPs are the major N_2O emission hotspots. Stripping occurs during aeration and the produced N_2O is emitted into the atmosphere [13, 53].

As mentioned in section 2.3, our modeling concerning the N_2O stripping was based on the k_La approach. Moreover, it was enriched by the SE which acted as a coefficient describing the divergence of the model prediction (Eq. 4) with respect to ideality (SE=1). Eq. 4 simplifies the real stripping process by assuming the following: i) the air bubbles are always free of N_2O; their enrichment in N_2O is negligible as they rise up in the basin, ii) the liquid phase (as DO or N_2O concentration) has a homogeneous composition, and iii) the same k_La independently of the liquid depth. The combined effect of different DO levels and the highest influent S_{NH4} value tested (i.e. 40 mg L^{-1}) on the N_2O-EF under different SEs (i.e. 0, 0.1, 0.25, 0.5, 0.75, 1) was evaluated using the parameters by Hiatt and Grady [24]. It is presented in Fig. 5 for $N_2O\text{-}EF_{TOTAL}$ (i.e. considering both the N_2O stripped and the N_2O contained in the effluent) as well as for the $N_2O\text{-}EF_{GAS}$ (referring exclusively to the stripping contribution).

Under the application of the highest influent S_{NH4} value tested in this study (i.e. 40 mg L^{-1}), the trends were always similar and the maximum N_2O-EF was always observed for a DO around 1.2 mg L^{-1}. However, the maximum absolute values differed. In specific, the maximum $N_2O\text{-}EF_{GAS}$ values ranged from 0% (SE=0) to ~21.1% (SE=1), while the maximum $N_2O\text{-}EF_{TOTAL}$ values were between 6.3% (SE=0) and ~22% (SE=1). In other words, the SE increase led to a general rise in the EF. This was sharper in the beginning (SE: 0→0.1) and, then, more gradual (SE: 0.25→1) (Fig. 5). The observed trend reflects that a lower SE gives more chances for N_2O to

follow the denitrification pathway (reaction 4 of denitrification in Fig. 2), thus favouring its consumption instead of its stripping.

For each of the SE values tested, the N_2O-EF_{TOTAL} was always higher than the respective N_2O-EF_{GAS} one, but not significantly (Fig. 5). The latter showed that the N_2O stripping majorly contributed to the N_2O EF estimation. Only in the case of SE=0 (the hypothetical case of no stripping) the contribution of the dissolved N_2O was very significant. More importantly, our results indicated that the SE factor was a very significant contributor to the final EF results. Hence, a more detailed modeling of the stripping process in the future, avoiding the simplifications previously commented can potentially increase the accuracy in the EF prediction and prevent its overestimation.

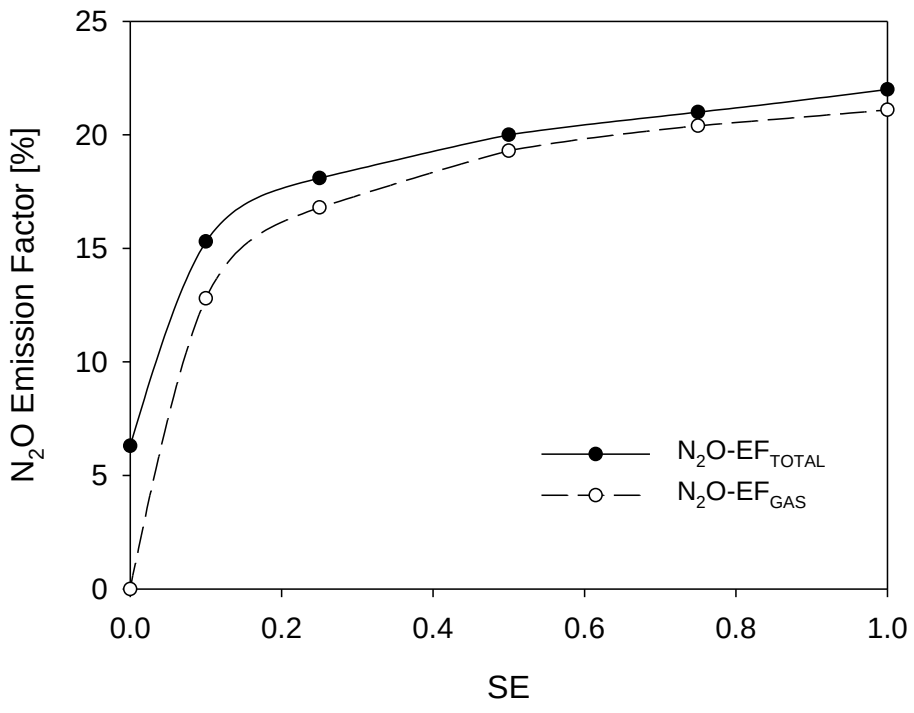

Figure 5. The maximum N_2O emission factor (N_2O-EF_{TOTAL} considering both the N_2O stripped and the N_2O contained in the effluent; N_2O-EF_{GAS} referring exclusively to the contribution of the N_2O stripping) observed for the different SE values (0, 0.1, 0.25, 0.5, 0.75, 1) tested during our simulations. The influent S_{NH4} value was considered equal to 40 mg L^{-1} and the parameters were retrieved from the study by Hiatt and Grady [24].

3.4 Modeling of dynamic N_2O emissions under disturbances

An additional goal of this work was to examine how the N_2O emissions were influenced by influent disturbances under different DO scenarios. Transition states after a disturbance are the most favourable scenarios for intermediates accumulation and, thus, higher N_2O emissions. As an example, the effect of a S_{NH4} concentration increase in the influent was studied (as a 'step' increase from 20 to 30 mgN L^{-1} on the 10th day of the plant operation). This was examined for various scenarios with different combinations of SE and DO control values in the aerobic reactor.

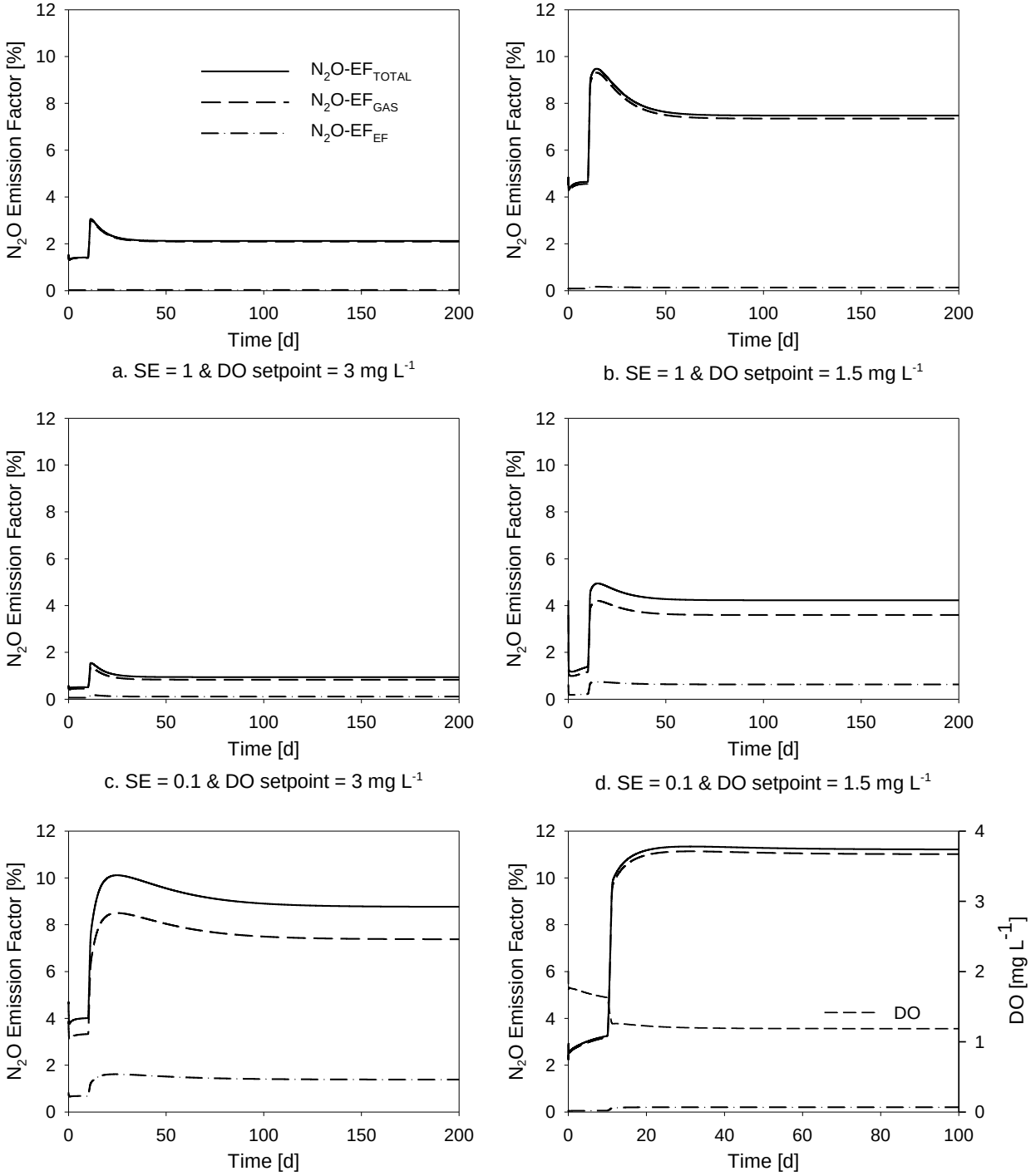

a. SE = 1 & DO setpoint = 3 mg L^{-1}

b. SE = 1 & DO setpoint = 1.5 mg L^{-1}

c. SE = 0.1 & DO setpoint = 3 mg L^{-1}

d. SE = 0.1 & DO setpoint = 1.5 mg L^{-1}

e. SE = 0.1 & DO setpoint = 1.2 mg L^{-1}

f. SE = 1 & no DO control

Figure 6. The effect of increasing the influent S_{NH4} concentration (from 20 to 30 mgN L^{-1}) at the 10th day of the plant operation on the N_2O-EF. Different SE values (1 and 0.1) and DO setpoints (3 mg L^{-1}, 1.5 mg L^{-1}, 1.2 mg L^{-1} and no DO control) were tested.

For the scenarios a and b, the SE was 1 to enable the observance of the full stripping effect under the sudden change of the operational conditions. The fast S_{NH4} increase resulted in a rapid increase of N_2O emissions. The N_2O-EF_{TOTAL} presented the following trends: 1.4→3.1% almost up to the 12th day of operation (scenario a) and 4.5→9.6% until the 17th day (scenario b). Then, a gradual EF reduction started until it was stabilized at lower levels: at ~2.1% after the 30th day (scenario a), and at ~7.5% after the 40th day (scenario b) (Fig. 6). The DO control setpoint in case b was significantly lower than in scenario a; thus, higher absolute EF values were expected as previously seen in Fig. 4A. Under such conditions, the AOB bacteria are known to induce nitritation, use NO_2^- as terminal electron acceptor and, finally, produce N_2O (nitrifier denitrification pathway) [54-56]. Indeed, low DO (e.g. <1.5 mg L^{-1}) has been experimentally connected with the achievement of nitritation, the subsequent NO_2^- accumulation and NOB washout [57-60]. For both scenarios a and b, the downward trend of the N_2O-EF indicated that NOB were growing and performing NO_2^- oxidation. However, the fact that the final N_2O-EF never recovered its initial value implies that the NOB growth only covered part of the new NO_2^- oxidation requirements. Fig. 7 shows the effect of scenarios a and b on the AOB and NOB growth. In both cases, the AOB growth was always sharper than the respective NOB one after the operational change on the 10th day. In accordance to what is seen in Fig. 7, the AOB population has been reported to prevail over the NOB under increased NH_4^+ availability and controlled aeration [61].

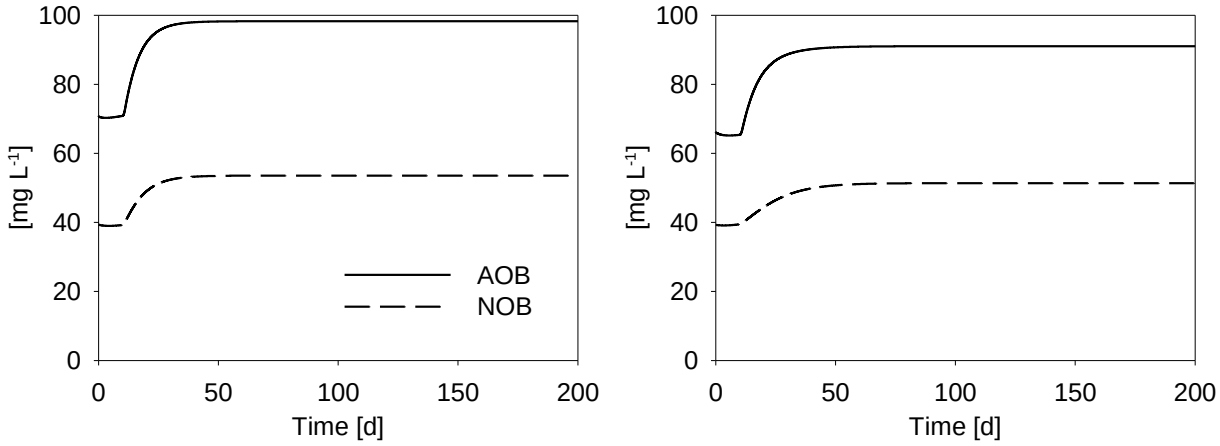

Figure 7. The AOB and NOB evolution after increasing the influent S_{NH4} concentration (from 20 to 30 mgN L^{-1}) on the 10th day of the plant operation. Different DO control setpoints (3 mg L^{-1} and 1.5 mg L^{-1}) were compared for a SE=1.

For the same DO levels, different SE values were tested to simulate the full and reduced stripping effect via fixing the SE as equal to 1 and 0.1, respectively (comparison between scenarios a and c, and comparison between scenarios b and d in Fig. 6). In terms of N_2O-EF_{TOTAL}, the same trends were observed: a fast increase followed by a decrease with a final value stabilized higher than the one observed before the S_{NH4} increase. The SE decrease (from 1 to 0.1) explains the increased distance between the lines of N_2O-EF_{TOTAL} and N_2O-EF_{GAS}. The emissions were lower in the SE=0.1 cases (Fig. 6c and 6d) and more N_2O was considered as remaining dissolved, thus coming out in the effluent. A lower SE value (i.e. 0.1) imposes less stripping to the system, which results in: i) an increased N_2O concentration in the aerobic reactor, and ii) an increased recycling of N_2O to the anoxic reactor leading to higher N_2O consumption.

Scenario e studies the effect of working at the DO setpoint of 1.2 mg·L^{-1} and SE =0.1, in order to show clearly the effect of working under DO conditions unfavorable to the NOB growth. N_2O emissions higher than 9% were observed because of N-removal via NO_2^- and NOB washout, as detailed in sections 3.1 and 3.2.

However, all the scenarios previously commented (i.e. scenarios a - e) were DO-controlled; this enabled simulating how increasing aeration by the control loop allowed the maintenance of the desired DO concentration. Scenario f, though, showed that the effect of the S_{NH4} influent increase can be higher and more persistent in a non-DO-controlled environment. The increase of NH_4^+ load decreases the DO concentration, and can move the system from an operational point with full nitrification to a point with N-removal via NO_2^- which explains the higher EF noted.

A sudden operational change imposed to the system such as the one examined in this section (i.e. a step increase in the influent S_{NH4} from 20 to 30 mg L^{-1}) increased the N_2O emissions. The AOB and NOB populations were affected, with the AOB growth being quicker and higher compared to the respective NOB one. Thus, N-removal via NO_2^- was increased and N_2O was produced through nitrifier denitrification. The magnitude of the emissions depended on the imposed SE value and DO control setpoint; the higher the imposed SE value, the higher the stripping effect and, thus, the anticipated emissions. Moreover, a lower DO setpoint placed the system under nitritation regime, thus creating the conditions for the activation of the nitrifier denitrification pathway. Under no DO control, the environment within the reactor became even more favorable to N-removal via NO_2^-, hence greatly increasing the EF.

3.5 Sensitivity Analysis (SA) of the developed model

Table 2 shows the 40 most sensitive parameters to the N_2O-EF_{TOTAL} for the two studied scenarios with influent S_{NH4}=30 mg L^{-1} and SE=0.5 (first: DO in the aerobic reactor=3 mg L^{-1}; second: DO in the aerobic reactor=1 mg L^{-1}). The values are listed in descending order considering the $S_{i,j}$ absolute values calculated with Eq. 6. The sign of the sensitivity indices is maintained since it contains information: a positive sensitivity index indicates that an increase in the parameter results in an increase of the N_2O-EF_{TOTAL}, while a negative sensitivity suggests that an increase in the parameter will lead to a decrease in the N_2O-EF_{TOTAL}. The results showed in Table 2 were obtained with a perturbation factor of 0.01%. The choice on the perturbation factor was based on the work by De Pauw [62] who suggested to use a factor producing equal derivative values for forward and backward differences. Nevertheless, the perturbation factor did not significantly affect the parameter categorization (data not shown).

Table 2. Sensitivity analysis results for the two different operational modes (first: DO_{AE} =3 mg L^{-1}; second: DO_{AE} =1 mg L^{-1}); both with influent S_{NH4}=30 mg L^{-1} and SE=0.5. DO_{AE} stands for the DO control setpoint in the aerobic reactor.

Order	**DO_{AE}=3 mg L^{-1}**		**DO_{AE}=1 mg L^{-1}**	
	Parameter	**Si,j**	**Parameter**	**Si,j**
1	μ_{NOB}	-2.138	Y_{AOB}	2.233
2	η_G	1.489	η_G	1.978
3	b_{NOB}	1.059	q_{AOB_AMO}	1.407
4	$q_{AOB\_N2O\_ND}$	0.997	Y_{PAO}	1.108
5	μ_{AOB_HAO}	-0.926	b_{AOB}	-1.024
6	$K_{I\_O2\_AOB}$	0.878	η_{G5}	-0.947
7	Y_{AOB}	0.863	K_{OH5}	-0.853
8	K_{HNO2_AOB}	-0.857	$q_{AOB\_N2O\_ND}$	0.841
9	K_{NO2_NOB}	0.851	K_{O2_AOB1}	-0.738

Order	DO_{AE}=3 mg L^{-1}		DO_{AE}=1 mg L^{-1}	
	Parameter	**Si,j**	**Parameter**	**Si,j**
10	Y_{PAO}	0.739	i_{NXS}	0.674
11	K_{O2_NOB}	0.629	Y_H	-0.470
12	η_{G5}	-0.620	Y_{PO4}	-0.435
13	K_{OH5}	-0.470	q_{PP}	0.400
14	K_{N2O_Den}	0.435	μ_{PAO}	-0.386
15	i_{NXS}	0.428	i_{NBM}	-0.375
16	b_{PAO}	-0.408	K_{HNO2_AOB}	-0.360
17	SE	0.375	i_{NSF}	0.338
18	Y_H	-0.364	$K_{I\_O2\_AOB}$	0.299
19	K_{MAX_P}	0.259	K_{MAX_P}	0.292
20	i_{NBM}	-0.247	SE	0.223
21	μ_{PAO}	0.246	K_{NH2OH_AOB}	-0.209
22	i_{NSF}	0.207	$K_{O2\_AOB\_ND}$	0.198
23	$K_{O2\_AOB\_ND}$	0.192	μ_{AOB_HAO}	-0.175
24	D_{O2}	-0.187	K_{N2O_Den}	0.170
25	D_{N2O}	-0.187	K_{S5}	0.166
26	K_{P_P}	-0.169	K_F	-0.157
27	K_{O2_AOB2}	0.167	Y_{PHA}	-0.149
28	K_{S5}	0.151	K_{NH4_AOB}	-0.137
29	b_H	0.149	n_{fe_H}	-0.134
30	Y_{PO4}	-0.135	K_{O2_P}	-0.132
31	K_{P_NOB}	0.122	b_H	0.121
32	q_{AOB_AMO}	-0.120	D_{O2}	-0.111
33	q_{PHA}	0.118	D_{N2O}	-0.111
34	K_H	-0.101	b_{PAO}	-0.101
35	K_F	-0.099	K_H	-0.098
36	n_{fe_H}	-0.094	k_La	0.089
37	Y_{PHA}	-0.094	K_{O2_AOB2}	0.082
38	q_{PP}	0.085	K_{IPP_P}	-0.074
39	η_{G3}	0.077	i_{PXS}	-0.073
40	i_{PXS}	-0.064	b_{PP}	-0.071

Different parameter ranking was found between the two scenarios: the most sensitive parameters to the N_2O-EF_{TOTAL} factor varied under the different DO setpoints. For the DO setpoint of 3 mg L^{-1}, the most sensitive parameters were those related to NOB metabolism, followed by those

related to the AOB activity and, finally, by those connected to PAO. The sensitivity of parameters referring to the NOB metabolism is important to understand potential NO_2^- accumulation. The latter will inevitably lead to changes in the total N_2O emission factor through the activation/deactivation of the nitrifier denitrification pathway, as discussed in section 3.1. On the other hand, under the DO setpoint of 1 mg L^{-1}, the AOB-related parameters were the most sensitive since limited NOB growth is anticipated in a low-DO environment (Fig. 3B). Hence, the NOB-related parameters became insensitive. For this scenario, the WWTP model operates under nitritation and increased N_2O production through nitrifier denitrification is expected (section 3.1).

For both tested scenarios, the anoxic growth factor (η_G) (i.e. the stoichiometric factor implicated in the growth of heterotrophs and PAO under anoxic conditions) had a severe impact on the N_2O emission factor. Considering that this parameter affects all the anoxic processes, its perturbation will change the stoichiometry of various processes.

It is worth mentioning that the SE only appears in the middle range of the table (17th and 20th for a DO setpoint of 3 and 1 mg L^{-1}, respectively). The reference value of this parameter (0.5) is essential to understand the sensitivity results. According to Fig. 5, the SE parameter has a significant effect on the $N_2O\text{-}EF_{TOTAL}$ while increasing from 0 to 0.2; its further increase from 0.2 to 1 has a lesser influence on the N_2O-EF values. Had this parameter been set at a lower value, its relative sensitivity would have increased.

Moreover, the conversion factors mostly affecting the $N_2O\text{-}EF_{TOTAL}$ were those related to the N-content (i_{NXS}, i_{NSF}) of state variables X_S and S_F. The latter can be justified by their interference in the calculation of the N_{IN} content (Eq. 2) and their subsequent effect on the $N_2O\text{-}EF_{TOTAL}$ estimation (Eq. 1.1).

Finally, we examined Table 2 again to see if any common parameters appeared in the first ten places for both scenarios. It was noted that n_G, $q_{AOB\_N2O\_ND}$ (maximum N_2O production rate by the nitrifier denitrification pathway), Y_{PAO} (yield coefficient for the PAO) and Y_H (yield coefficient for the heterotrophs) were amongst the first ten parameters for both DO setpoints; all with positive sensitivity. Hence, it can be deduced that decreasing these values leads to a decrease in the N_2O-EF_{TOTAL}. The n_G, Y_{PAO} and Y_H stoichiometric parameters, in specific, are included in the stoichiometry of the processes referring to the anoxic growth of PAO and heterotrophs. These processes can indeed be considered as significantly influencing the EF since they occur in an anoxic environment where N_2O can be consumed through denitrification. These results also show that the inclusion of PAO in our model has a significant impact in the EF related to the denitrification of N_2O. Lastly, the impact of the $q_{AOB\_N2O\_ND}$ kinetic parameter proved to be important in both scenarios. Given that $q_{AOB\_N2O\_ND}$ expresses the N_2O production rate through nitrifier denitrification, this observation indicates that nitrifier denitrification is probably the most important pathway to consider for the N_2O mitigation.

4. Conclusions

In this work, an ASM2d-N_2O model including COD, N and P removal along with all the known N_2O microbial pathways was developed for a municipal A^2/O WWTP, which can be highly useful for the estimation of the N_2O-EF. The following major conclusions were reached:

- Plant operators often opt for lower aeration to decrease a WWTP's energy requirements. With the aerobic DO ranging from 0.8 to 1.8 mg L^{-1}, the AOB prevailed over the NOB, thus promoting the shift from full to partial nitrification and, subsequently, the N_2O

production through nitrifier denitrification. Due to the important N_2O GWP, this operational change can result in a high final overall WWTP carbon footprint. Consequently, low aeration is desired only if it does not disturb the nitrification process.

- A SE coefficient (from 0 to 1) was added to reflect the non-ideality of the stripping modeling. Decreasing the SE was translated into higher N_2O concentration in the mixed liquor; the latter led to a higher N_2O denitrification rate and lower emissions.
- The effect of a sudden increase in the influent S_{NH4} from 20 to 30 mg L^{-1} was simulated. The AOB predominance over the NOB enabled NO_2^- accumulation and increased the nitrifier denitrification pathway. Higher emissions were observed under the following conditions: lower DO setpoints that created an environment more advantageous to nitrifier denitrification combined with higher SE values that raised the significance of the stripping effect.
- The sensitivity analysis showed that the NOB-related parameters had minor influence over the N_2O-EF under low-DO conditions, given the limited NOB growth at low DO. However, they were very significant at high DO due to its effect on the NO_2^- oxidation rate. The parameters n_G, $q_{AOB\_N2O\_ND}$, Y_{PAO} and Y_H were amongst the top ten for both DO setpoints tested. n_G, Y_{PAO} and Y_H are related to the N_2O consumption through denitrification. $q_{AOB\_N2O\_ND}$ indicates that nitrifier denitrification is probably the most important pathway to consider for the N_2O mitigation.

Acknowledgments

This project has received funding from the European Union's Horizon 2020 research and innovation program under the Marie Skłodowska-Curie C-FOOT-CTRL project (grant agreement No 645769). T.M. Massara is also grateful to the Natural Environment Research Council (NERC) of the UK for the 4-year full PhD studentship. B. Solís also acknowledges the support of Universitat Autònoma de Barcelona with a PIF pre-doctoral grant. J.A. Baeza, A. Guisasola and B. Solís are members of the GENOCOV research group (*Grup de Recerca Consolidat de la Generalitat de Catalunya*, 2014 SGR 1255).

References

[1] IPCC, Climate change 2013: the physical science basis. Contribution of Working Group I to the Fifth Assessment Report of the Intergovernmental Panel on Climate Change, in: T.F. Stocker, D. Qin, G.K. Plattner, M. Tignor, S.K. Allen, J. Boschung, A. Nauels, Y. Xia, V. Bex, P.M. Midgley (Eds.), Cambridge University Press, Cambridge and New York, 2013, pp. 1535.

[2] A.R. Ravishankara, J.S. Daniel, R.W. Portmann, Nitrous Oxide (N_2O): The Dominant Ozone-Depleting Substance Emitted in the 21st Century, Science 326 (2009) 123 LP-125. http://science.sciencemag.org/content/326/5949/123.abstract.

[3] J.H. Ahn, S. Kim, H. Park, B. Rahm, K. Pagilla, K. Chandran, N_2O emissions from activated sludge processes, 2008-2009: results of a national monitoring survey in the United States., Environ. Sci. Technol. 44 (2010) 4505–4511. doi:10.1021/es903845y.

[4] J. Foley, D. de Haas, Z. Yuan, P. Lant, Nitrous oxide generation in full-scale biological nutrient removal wastewater treatment plants, Water Res. 44 (2010) 831-844. doi:10.1016/j.watres.2009.10.033.

[5] A. Rodríguez-Caballero, I. Aymerich, R. Marques, M. Poch, M. Pijuan, Minimizing N_2O emissions and carbon footprint on a full-scale activated sludge sequencing batch reactor, Water Res. 71 (2015) 1-10. doi:10.1016/j.watres.2014.12.032.

[6] M.R.J. Daelman, B. De Baets, M.C.M. van Loosdrecht, E.I.P. Volcke, Influence of sampling strategies on the estimated nitrous oxide emission from wastewater treatment plants, Water Res. 47 (2013) 3120-3130. doi:10.1016/j.watres.2013.03.016.

[7] P. Wunderlin, J. Mohn, A. Joss, L. Emmenegger, H. Siegrist, Mechanisms of N_2O production in biological wastewater treatment under nitrifying and denitrifying conditions, Water Res. 46 (2012) 1027-1037. doi:10.1016/j.watres.2011.11.080.

[8] P. Wunderlin, M.F. Lehmann, H. Siegrist, B. Tuzson, A. Joss, L. Emmenegger, J. Mohn, Isotope Signatures of N_2O in a Mixed Microbial Population System: Constraints on N_2O Producing Pathways in Wastewater Treatment, Environ. Sci. Technol. 47 (2013) 1339-1348. doi:10.1021/es303174x.

[9] B.J. Ni, Z. Yuan, Recent advances in mathematical modeling of nitrous oxides emissions from wastewater treatment processes, Water Res. 87 (2015) 336-346. doi:10.1016/j.watres.2015.09.049.

[10] M.J. Kampschreur, H. Temmink, R. Kleerebezem, M.S.M. Jetten, M.C.M. van Loosdrecht, Nitrous oxide emission during wastewater treatment, Water Res. 43 (2009) 4093-4103. doi:10.1016/j.watres.2009.03.001.

[11] J. Desloover, S.E. Vlaeminck, P. Clauwaert, W. Verstraete, N. Boon, Strategies to mitigate N_2O emissions from biological nitrogen removal systems, Curr. Opin. Biotechnol. 23 (2012) 474-482. doi:10.1016/j.copbio.2011.12.030.

[12] T.M. Massara, S. Malamis, A. Guisasola, J.A. Baeza, C. Noutsopoulos, E. Katsou, A review on nitrous oxide (N_2O) emissions during biological nutrient removal from municipal wastewater and sludge reject water, Sci. Total Environ. 596-597 (2017) 106-123. doi:10.1016/j.scitotenv.2017.03.191.

[13] Y. Law, L. Ye, Y. Pan, Z. Yuan, Nitrous oxide emissions from wastewater treatment processes., Philos. Trans. R. Soc. Lond. B. Biol. Sci. 367 (2012) 1265-77. doi:10.1098/rstb.2011.0317.

[14] R. Marques, A. Rodríguez-Caballero, A. Oehmen, M. Pijuan, Assessment of online monitoring strategies for measuring N_2O emissions from full-scale wastewater treatment systems, Water Res. 99 (2016) 171-179. doi:10.1016/j.watres.2016.04.052.

[15] Y. Lim, D.-J. Kim, Quantification method of N_2O emission from full-scale biological nutrient removal wastewater treatment plant by laboratory batch reactor analysis., Bioresour. Technol. 165 (2014) 111-115. doi:10.1016/j.biortech.2014.03.021.

[16] A. Rodríguez-Caballero, I. Aymerich, M. Poch, M. Pijuan, Evaluation of process conditions triggering emissions of green-house gases from a biological wastewater treatment system, Sci. Total Environ. 493 (2014) 384-391. doi:10.1016/j.scitotenv.2014.06.015.

[17] M. Pocquet, Z. Wu, I. Queinnec, M. Spérandio, A two pathway model for N_2O emissions by ammonium oxidizing bacteria supported by the NO/N_2O variation, Water Res. 88 (2016) 948-959. doi:10.1016/j.watres.2015.11.029.

[18] B.-J. Ni, M. Ruscalleda, C. Pellicer-Nàcher, B.F. Smets, Modeling Nitrous Oxide Production during Biological Nitrogen Removal via Nitrification and Denitrification: Extensions to the General ASM Models, Environ. Sci. Technol. 45 (2011) 7768-7776. doi:10.1021/es201489n.

[19] K.E. Mampaey, B. Beuckels, M.J. Kampschreur, R. Kleerebezem, M.C.M. van Loosdrecht, E.I.P. Volcke, Modelling nitrous and nitric oxide emissions by autotrophic ammonia-oxidizing bacteria, Environ. Technol. 34 (2013) 1555-1566. doi:10.1080/09593330.2012.758666.

[20] Y. Law, B.J. Ni, P. Lant, Z. Yuan, N_2O production rate of an enriched ammonia-oxidising bacteria culture exponentially correlates to its ammonia oxidation rate, Water Res. 46 (2012) 3409-3419. doi:10.1016/j.watres.2012.03.043.

[21] B.-J. Ni, L. Ye, Y. Law, C. Byers, Z. Yuan, Mathematical modeling of nitrous oxide (N_2O) emissions from full-scale wastewater treatment plants., Environ. Sci. Technol. 47 (2013) 7795-7803. doi:10.1021/es4005398.

[22] K. Chandran, L.Y. Stein, M.G. Klotz, M.C.M. van Loosdrecht, Nitrous oxide production by lithotrophic ammonia-oxidizing bacteria and implications for engineered nitrogen-removal systems, Biochem. Soc. Trans. 39 (2011) 1832 LP-1837. http://www.biochemsoctrans.org/content/39/6/1832.abstract.

[23] B.-J. Ni, L. Peng, Y. Law, J. Guo, Z. Yuan, Modeling of Nitrous Oxide Production by Autotrophic Ammonia-Oxidizing Bacteria with Multiple Production Pathways, Environ. Sci. Technol. 48 (2014) 3916-3924. doi:10.1021/es405592h.

[24] W.C. Hiatt, C.P.L. Grady, An updated process model for carbon oxidation, nitrification, and denitrification., Water Environ. Res. 80 (2008) 2145-2156. doi:10.2175/106143008X304776.

[25] Y. Pan, B.J. Ni, Z. Yuan, Modeling electron competition among nitrogen oxides reduction and N_2O accumulation in denitrification, Environ. Sci. Technol. 47 (2013) 11083-11091. doi:10.1021/es402348n.

[26] B.J. Ni, Y. Pan, B. Van Den Akker, L. Ye, Z. Yuan, Full-Scale Modeling Explaining Large Spatial Variations of Nitrous Oxide Fluxes in a Step-Feed Plug-Flow Wastewater Treatment Reactor, Environ. Sci. Technol. 49 (2015) 9176-9184. doi:10.1021/acs.est.5b02038.

[27] J. Guerrero, A. Guisasola, J.A. Baeza, The nature of the carbon source rules the competition between PAO and denitrifiers in systems for simultaneous biological nitrogen and phosphorus removal, Water Res. 45 (2011) 4793-4802. doi:10.1016/j.watres.2011.06.019.

[28] V.C. Machado, J. Lafuente, J.A. Baeza, Activated sludge model 2d calibration with full-scale WWTP data: Comparing model parameter identifiability with influent and operational uncertainty, Bioprocess Biosyst. Eng. 37 (2014) 1271-1287. doi:10.1007/s00449-013-1099-8.

[29] M. Henze, W. Gujer, T. Mino, M.C.M. van Loosdrecht, Activated Sludge Models ASM1, ASM2, ASM2d, and ASM3, IWA Scientific and Technical Report n.9., IWA Publishing, London, 2000.

[30] I. Takács, G.G. Patry, D. Nolasco, A dynamic model of the clarification-thickening process, Water Res. 25 (1991) 1263-1271. doi:10.1016/0043-1354(91)90066-Y.

[31] I. Jubany, J. Carrera, J. Lafuente, J.A. Baeza, Start-up of a nitrification system with automatic control to treat highly concentrated ammonium wastewater: Experimental results and modeling, Chem. Eng. J. 144 (2008) 407-419. doi:10.1016/j.cej.2008.02.010.

[32] S. Capela, M. Roustan, A. Heduit, Transfer number in fine bubble diffused aeration systems, Water Sci. Technol. 43 (2001) 145-152.

[33] D.R. Lide, CRC Handbook of Chemistry and Physics, 87th ed., CRC Press/Taylor and Francis Group, Boca Raton, 2007.

[34] H. Hauduc, L. Rieger, I. Takács, A. Héduit, P.A. Vanrolleghem, S. Gillot, A systematic approach for model verification: application on seven published activated sludge models, Water Sci. Technol. 61(2010) 825-839. doi: 10.2166/wst.2010.898

[35] P. Reichert, P.A. Vanrolleghem, Identifiability and uncertainty analysis of the river water quality model no. 1 (RWQM1), Water Sci. Technol. 43 (2001) 329-338.

[36] U. Wiesmann, Biological nitrogen removal from wastewater, in: A. Fiechter (Eds.), Advances in Biochemical Engineering Bio- technology, Springer-Verlag, Berlin, 1994, pp. 113-154.

[37] A. Guisasola, M. Marcelino, R. Lemaire, J.A. Baeza, Z. Yuan, Modelling and simulation revealing mechanisms likely responsible for achieving the nitrite pathway through aeration control, Water Sci. Technol. 61 (2010) 1459-1465. doi: 10.2166/wst.2010.017

[38] G. Tallec, J. Garnier, G. Billen, M. Gousailles, Nitrous oxide emissions from secondary activated sludge in nitrifying conditions of urban wastewater treatment plants: Effect of oxygenation level, Water Res. 40 (2006) 2972-2980. doi:10.1016/j.watres.2006.05.037.

[39] M.J. Kampschreur, W.R.L. van der Star, H.A. Wielders, J.W. Mulder, M.S.M. Jetten, M.C.M. van Loosdrecht, Dynamics of nitric oxide and nitrous oxide emission during full-scale reject water treatment, Water Res. 42 (2008) 812-826. doi:10.1016/j.watres.2007.08.022.

[40] Y. Law, P. Lant, Z. Yuan, The confounding effect of nitrite on N_2O production by an enriched ammonia-oxidizing culture, Environ. Sci. Technol. 47 (2013) 7186-7194. doi:10.1021/es4009689.

[41] L. Peng, B.J. Ni, D. Erler, L. Ye, Z. Yuan, The effect of dissolved oxygen on N_2O production by ammonia-oxidizing bacteria in an enriched nitrifying sludge, Water Res. 66 (2014) 12-21. doi:10.1016/j.watres.2014.08.009.

[42] A. Aboobakar, E. Cartmell, T. Stephenson, M. Jones, P. Vale, G. Dotro, Nitrous oxide emissions and dissolved oxygen profiling in a full-scale nitrifying activated sludge treatment plant, Water Res. 47 (2013) 524-534. doi:10.1016/j.watres.2012.10.004.

[43] G. Dotro, B. Jefferson, M. Jones, P. Vale, E. Cartmell, T. Stephenson, A review of the impact and potential of intermittent aeration on continuous flow nitrifying activated sludge, Environ. Technol. 32 (2011) 1685-1697. doi:10.1080/09593330.2011.597783.

[44] I. Jubany, J. Lafuente, J.A. Baeza, J. Carrera, Total and stable washout of nitrite oxidizing bacteria from a nitrifying continuous activated sludge system using automatic control based on Oxygen Uptake Rate measurements, Water Res. 43 (2009) 2761-2772. doi:10.1016/j.watres.2009.03.022.

[45] O. Turk, D.S. Mavinic, Benefits of using selective inhibition to remove nitrogen from highly nitrogenous wastes, Environ. Technol. Lett. 8 (1987) 419-426. doi:10.1080/09593338709384500.

[46] Y. Peng, G. Zhu, Biological nitrogen removal with nitrification and denitrification via nitrite pathway, Appl. Microbiol. Biotechnol. 73 (2006) 15-26. doi:10.1007/s00253-006-0534-z.

[47] G. Ruiz, D. Jeison, R. Chamy, Nitrification with high nitrite accumulation for the treatment of wastewater with high ammonia concentration, Water Res. 37 (2003) 1371-1377.

[48] A. Guisasola, I. Jubany, J.A. Baeza, J. Carrera, J. Lafuente, Respirometric estimation of the oxygen affinity constants for biological ammonium and nitrite oxidation, J. Chem. Technol. Biotechnol. 80 (2005) 388-396. doi:10.1002/jctb.1202.

[49] M. Soliman, A. Eldyasti, Development of partial nitrification as a first step of nitrite shunt process in a Sequential Batch Reactor (SBR) using Ammonium Oxidizing Bacteria (AOB)

controlled by mixing regime, Bioresour. Technol. 221 (2016) 85-95. doi:10.1016/j.biortech.2016.09.023.

[50] M. Pijuan, J. Torà, A. Rodríguez-Caballero, E. César, J. Carrera, J. Pérez, Effect of process parameters and operational mode on nitrous oxide emissions from a nitritation reactor treating reject wastewater, Water Res. 49 (2014) 23-33. doi:10.1016/j.watres.2013.11.009.

[51] R.M.L.D. Rathnayake, M. Oshiki, S. Ishii, T. Segawa, H. Satoh, S. Okabe, Effects of dissolved oxygen and pH on nitrous oxide production rates in autotrophic partial nitrification granules, Bioresour. Technol. 197 (2015) 15-22. doi:10.1016/j.biortech.2015.08.054.

[52] N. Frison, A. Chiumenti, E. Katsou, S. Malamis, D. Bolzonella, F. Fatone, Mitigating off-gas emissions in the biological nitrogen removal via nitrite process treating anaerobic effluents, J. Clean. Prod. 93 (2015) 126-133. doi:http://dx.doi.org/10.1016/j.jclepro.2015.01.017.

[53] G. Mannina, A. Cosenza, D. Di Trapani, V.A. Laudicina, C. Morici, H. Ødegaard, Nitrous oxide emissions in a membrane bioreactor treating saline wastewater contaminated by hydrocarbons, Bioresour. Technol. 219 (2016) 289-297. doi:10.1016/j.biortech.2016.07.124.

[54] J.G. Kuenen, Anammox bacteria: from discovery to application., Nat. Rev. Microbiol. 6 (2008) 320-326. doi:10.1038/nrmicro1857.

[55] L. Peng, B.-J. Ni, L. Ye, Z. Yuan, The combined effect of dissolved oxygen and nitrite on N_2O production by ammonia oxidizing bacteria in an enriched nitrifying sludge, Water Res. 73 (2015) 29-36. doi:10.1016/j.watres.2015.01.021.

[56] Y. Jin, D. Wang, W. Zhang, Effects of substrates on N_2O emissions in an anaerobic ammonium oxidation (anammox) reactor, Springerplus. (2016) 1-12. doi:10.1186/s40064-016-2392-1.

[57] J.M. Garrido, W.A.J. Van Benthum, M.C.M. Van Loosdrecht, J.J. Heijnen, Influence of dissolved oxygen concentration on nitrite accumulation in a biofilm airlift suspension reactor, Biotechnol. Bioeng. 53 (1997) 168-178. doi:10.1002/(SICI)1097-0290(19970120)53:2<168::AID-BIT6>3.0.CO;2-M.

[58] W. Bae, S. Baek, J. Chung, Y. Lee, Optimal operational factors for nitrite accumulation in batch reactors, Biodegradation. 12 (2001) 359-366. doi:10.1023/A:1014308229656.

[59] G. Ciudad, O. Rubilar, P. Muñoz, G. Ruiz, R. Chamy, C. Vergara, D. Jeison, Partial nitrification of high ammonia concentration wastewater as a part of a shortcut biological nitrogen removal process, Process Biochem. 40 (2005) 1715-1719. doi:10.1016/j.procbio.2004.06.058.

[60] R. Blackburne, Z. Yuan, J. Keller, Partial nitrification to nitrite using low dissolved oxygen concentration as the main selection factor, Biodegradation. 19 (2008) 303-312. doi:10.1007/s10532-007-9136-4.

[61] M. Pan, Z. Hu, R. Liu, X. Zhan, Effects of loading rate and aeration on nitrogen removal and N_2O emissions in intermittently aerated sequencing batch reactors treating slaughterhouse wastewater at 11 ºC, Bioprocess Biosyst. Eng. 38 (2015) 681-689. doi:10.1007/s00449-014-1307-1.

[62] D.J.W. De Pauw, Optimal Experimental Design for Calibration of Bioprocess Models: A Validated Software Toolbox, PhD thesis in Applied Biological Sciences, University of Gent, Belgium. http://biomath.urgent.be/publications/download/, 2005 (accessed 17.06.17).

Figure 2

Click here to download high resolution image

AOB

1. $NH_4^+ + \frac{1}{2} O_2 \xrightarrow[AMO]{} NH_2OH + H^+$

2. $NH_2OH + \frac{3}{4} O_2 + i_{NBM}\ NH_4^+ \xrightarrow[HAO]{} NO + 3/2\ H_2O + X_{AOB}$

3. $NO + \frac{1}{4} O_2 + \frac{1}{2} H_2O \xrightarrow[HAO]{} NO_2^- + H^+$

4. $NH_2OH + 4\ NO \xrightarrow[Nor]{} NO_2^- + 2\ N_2O + H_2O + H^+$ **NH_2OH oxidation pathway**

5a. $NH_2OH + 3\ NO_2^- + 3\ H^+ \rightarrow 4\ NO + 3\ H_2O$

5b. $NH_2OH + 2\ NO \rightarrow 3/2\ N_2O + 3/2\ H_2O$

(5a + 2 * 5b)/3 = 5

5. $NH_2OH + NO_2^- + H^+ \xrightarrow[NirK + Nor]{} N_2O + 2\ H_2O$ **Nitrifier denitrification pathway**

Heterotrophic Denitrifiers

1. $NO_3^- + 2\ e^- + 2\ H^+ \xrightarrow[NaR]{} NO_2^- + H_2O$

2. $NO_2^- + e^- + 2\ H^+ \xrightarrow[NiR]{} NO + H_2O$

3. $NO + e^- + H^+ \xrightarrow[NOR]{} \frac{1}{2} N_2O + \frac{1}{2} H_2O$ **Heterotrophic denitrification pathway**

4. $\frac{1}{2} N_2O + e^- + H^+ \xrightarrow[N_2OR]{} \frac{1}{2} N_2 + \frac{1}{2} H_2O$

Figure 3
Click here to download high resolution image

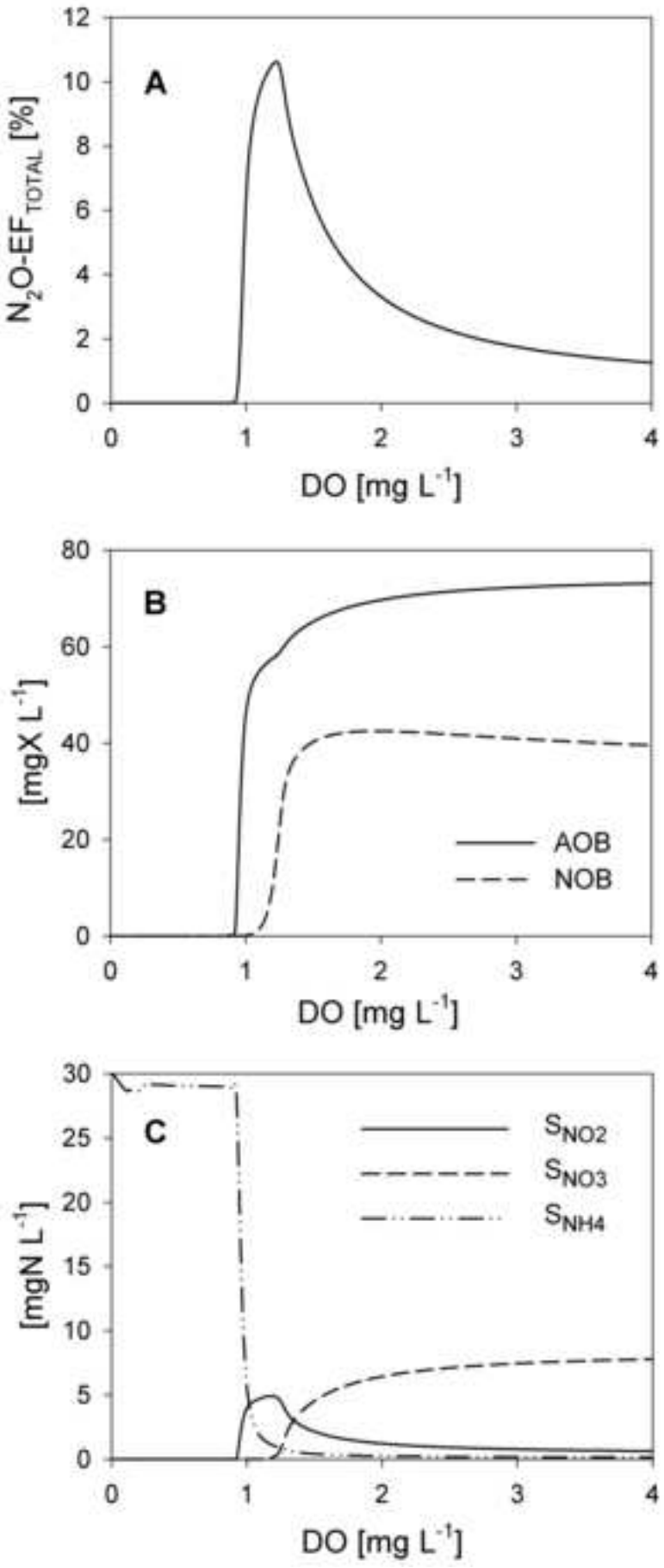

Figure 4
Click here to download high resolution image

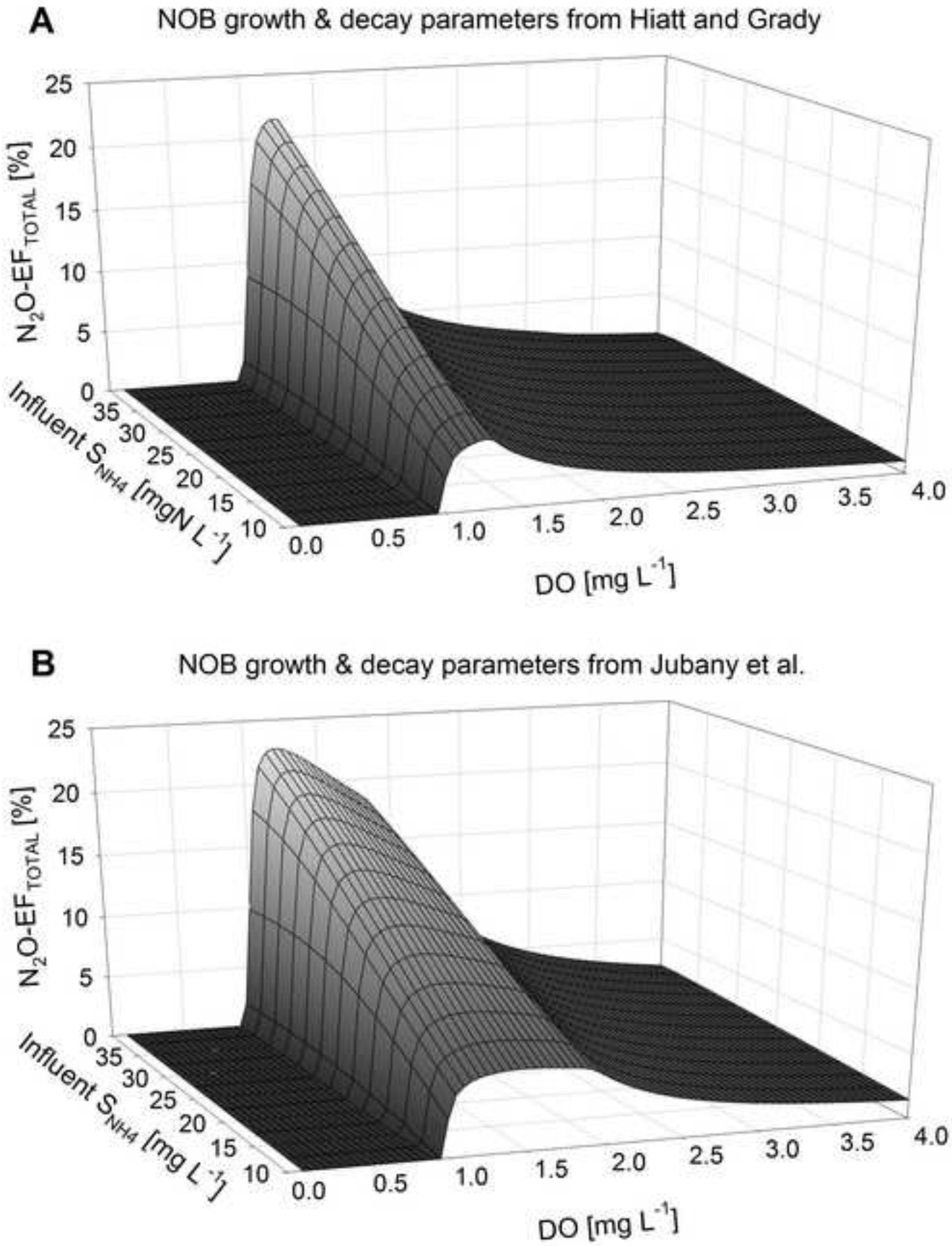

Figure 5
Click here to download high resolution image

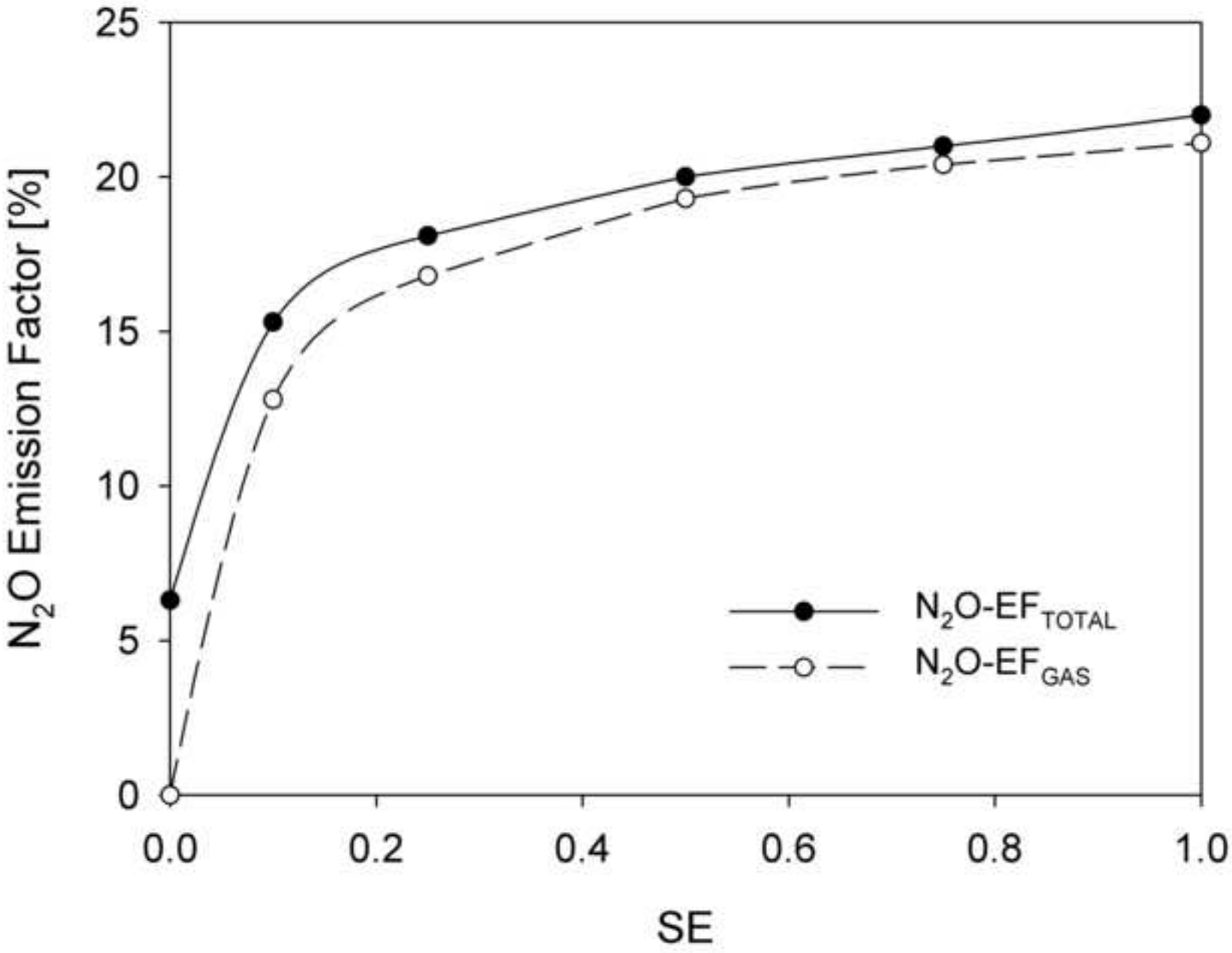

Figure 6

Click here to download high resolution image

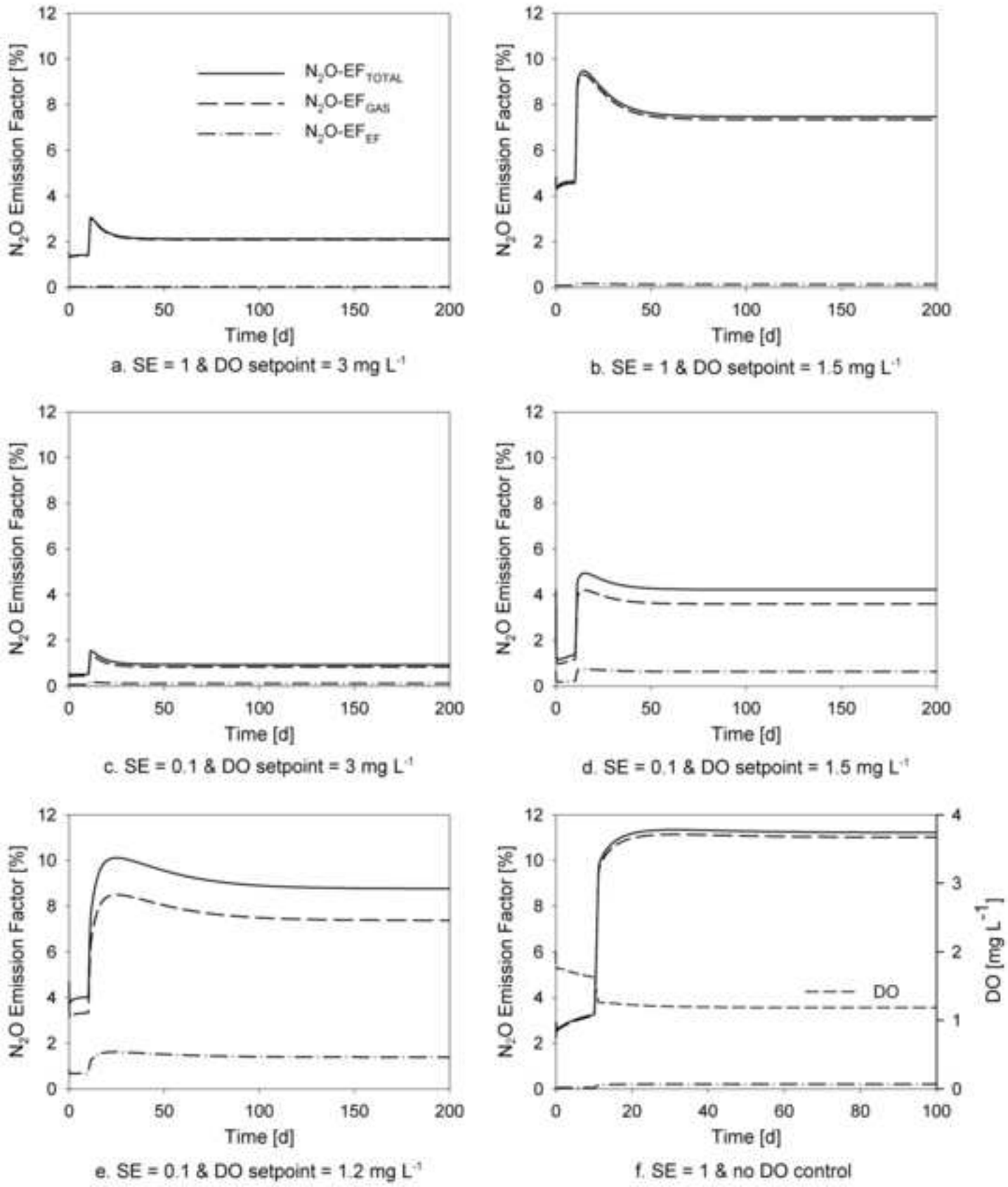

Figure 7
Click here to download high resolution image

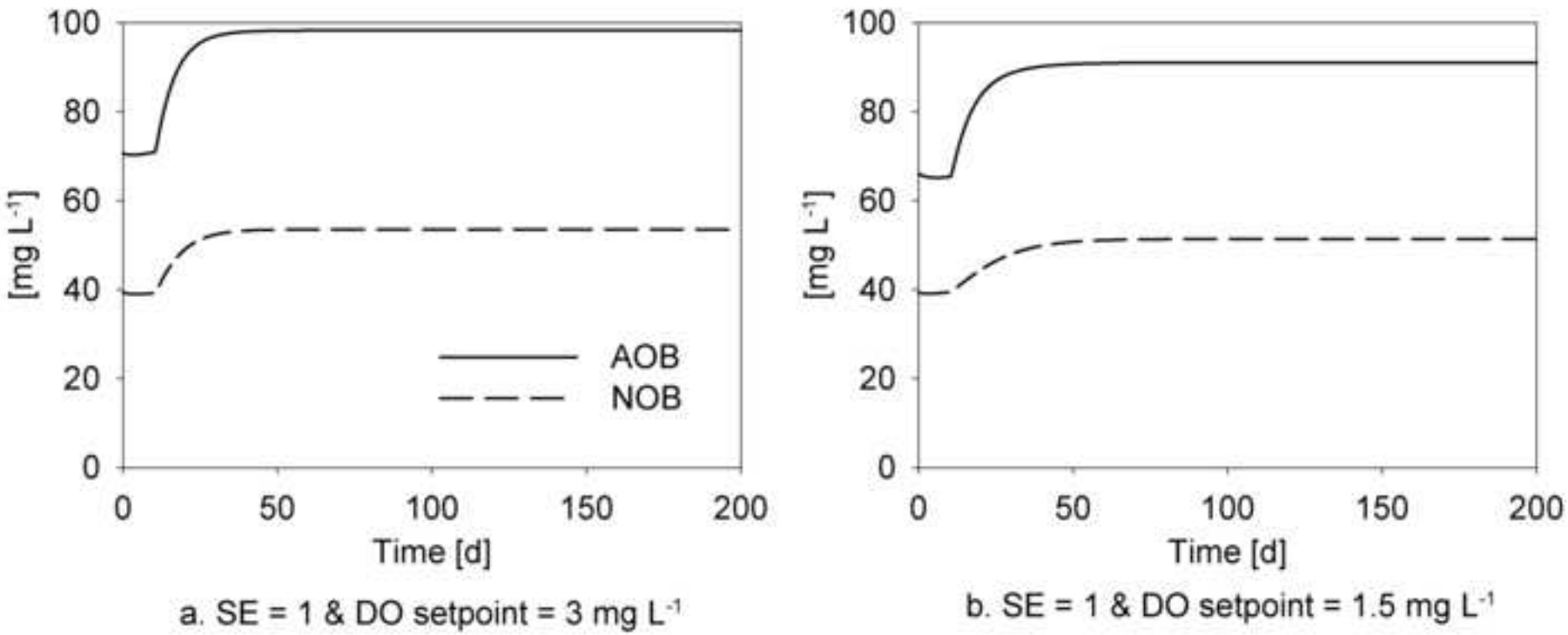

Supplementary Material

Click here to download Supplementary Material: ASM2d-N2O_Supportive Material_REVISED.pdf

Supplementary Material XLS

Click here to download Supplementary Material: ASM2d-N2O_Continuity Check Matrix.xlsx